Role of Unsaturated Soil Mechanics in Foundation Design

Allah Bahman Ibrahimi, MSc

Submitted in fulfillment of the requirements

for the degree of Master of Science

in Civil & Environmental Engineering

School of Engineering and Digital Sciences

Department of Civil & Environmental Engineering

Nazarbayev University

53 Kabanbay Batyr Avenue,

Astana, Kazakhstan, 010000

Supervisor: Professor Alfrendo Satyanaga

Co-Supervisor: Professor Sung Woo Moon

01/05/2023

Originality statement

By signing this document, I (Allah Bahman Ibrahimi) certify that this thesis is entirely original work of mine and has not been submitted in whole or in part for credit toward any other academic degree. I conducted the independent investigation and study that led to the work that is described in this thesis. All information sources used in this thesis have been properly cited and acknowledged. There has been no intentional plagiarism in this thesis or attempt to pass off someone else's work as my own. Except when I have explicitly credited others, all of the theories, concepts, and ideas I provide in this thesis are entirely mine. This thesis is a product of my independent research; it has not been purchased or outsourced.

Allah Bahman Ibrahimi 

TABLE OF CONTENT

List of Figure

List of Tables

Chapter 1 Introduction

1.1 Overview

It is well recognized that arid or semi-arid regions make up one-third of the earth's surface. Some places in these regions have unsaturated soil and a deep groundwater table. Three sub-layers make up the unsaturated zone, which is visible above the groundwater table and below the surface of the earth. The capillary zone is the topmost stratum above the groundwater. The two-phase zone is the name of the second stratum. The dry zone is the third stratum (Fredlund et.al 2011)

It is standard practice to always assume that the soil is saturated when designing foundations for locations in unsaturated soil (Vanapalli et al., 2007; Vanapalli et al., 2010) (Vanapalli et.al., 2012). Some factors, such as climate change, which is leading to an increase in rainfall intensity year-round, have an impact on the characteristics of unsaturated soil. Rainfall causes a drop in the negative pore-water pressure, shear strength, and soil strength in unsaturated soil. It is crucial to research how rainfall affects the mechanics of unsaturated soil for foundation design since rainfall reduces the shear strength of unsaturated soil (Jakariac et.al., 2013). To determine the shaft capacity of a pile foundation and to determine the shaft capacity of saturated soil, three formulae (α, β, and λ) are utilized (Vanapalli et.al., 2011). Based on saturated shear strength parameters and the soil-water characteristic curve (SWCC), these three formulae are adjusted to determine the fluctuation of the shaft capacity of pile foundation in unsaturated soil integrating matric suction (Vanapalli et al., 2007). For engineers to develop an understanding of the soil surface and boundary conditions, they must be able to forecast the flow of moisture in the soil. When planning foundations, paving, and slopes, the interaction between the soil and the surroundings must constantly be considered (Rahardjo et al., 2012). It is challenging to forecast and deal with the expansion modelling of the soil since environmental factors and water levels are continually changing (Morris et al., 1992).

One of the most significant indicators that convey information on the interaction of soil's water and solid phases is the soil SWCC, often known as the water retention curve (Rahardjo et al., 2016). SWCC is frequently utilized for both practical activities like optimizing sustainable agricultural production management and conducting research soil physical studies (Fredlund et al., 2011). The accuracy of the forecast, the suitability of the model and, consequently, the management of soil processes will all depend on how well this dependency is determined (Kim et al., 2012).

With the building of the major SWCC, many areas remain unexplored even though extensive databases of diverse soil properties have now been developed in Kazakhstan (Zhussupbekov et al., 2018). This is because the research and creation of these functions can take a long time. In particular, the connection between water content and suction, or the so-called soil-water characteristic curve, must be understood to comprehend the features of unsaturated soil for this area.

1.2 Objectives

There is negative pore water pressure (matric suction) and net normal stress within the unsaturated soil contributing to the additional shear strength of the soil. This benefits the practicing engineers in optimizing the design of the foundation which leads to the lower cost of a construction project. Therefore, the mechanics of unsaturated soil is necessary for the design of foundations under variations of rainfall loading. The objective of this study is related to the investigation of the importance of unsaturated soil mechanics in foundation design. The analytical calculation, laboratory testing, and numerical analyses were conducted in this study for the completion of the master thesis.

1.3 Thesis statement

- Effect of rainfall on characteristics of soils surrounding the foundation
- Shaft capacity of pile foundation due to the changes of moisture content in unsaturated soil properties

Chapter 2 Literature Review

When creating shallow foundations, it's imperative to take the shaft capacity and settling behavior into consideration. Even when unsaturated soils are still unsaturated, their shaft capacity and modulus of elasticity are often translated as if the soil is saturated. According to the accepted idea, a gradient of soil suction drives the flow of liquid in the soil (Kristo et al., 2019). It is among the most crucial elements of the mechanics of unsaturated soil. Soil suction is based on the concept of soil water potential, which compares the potential energy of soil water to that of pure water per unit of volume, mass, or weight (Rahardjo et al., 2016). A more conservative definition of soil suction is the difference between the pore-air pressure and pore-water pressure of the soil (u_a- u_w).

According to the accepted idea, a gradient of soil suction drives the flow of liquid in the soil (Rahardjo et al., 2018). The theory of soil water potential, which contrasts the potential energy of soil water to that of pure water per unit of volume, mass, or weight, serves as the foundation for understanding soil suction (Fredlund et al., 2011). The difference between the soil's pore-air pressure and pore-water pressure is a more conservative definition of soil suction. (ua - uw). The SWCC of soils, or the dependence of soil suction on soil moisture, is tied to the primary method for characterizing the flow of moisture, based on the application of the thermodynamic apparatus of soil moisture (Fredlund and Rahardjo, 1993). Modern ideas claim that the SWCC is a numerical measure of soils' ability to retain water (Zhai et al., 2019). The ability of soil to keep rainwater by soil suction is known as water retention. It may be measured as the amount of soil moisture at a specific pressure (Zhai et al., 2017). Increased soil moisture under persistent pressure may allow the soil to store more water (Zhai et al., 2012). Roads, embankments, and dams are a few geotechnical constructions that may be erected on or in compacted unsaturated soils with shallow or deep foundations. Pile foundations are also widely employed in fine- and coarse-grained soils found in natural sources where the groundwater table is deeper. The unsaturated soil zone above the groundwater table functions as a distribution point for the stresses associated with shallow and deep foundations under these conditions. Such situations are typical in semi-arid and dry regions of the world where pile foundations are employed to sustain huge loads and prevent settlements. The effect of matric suction or capillary stress on deep foundations' capacity to support loads is only slightly discussed in the literature (Douthitt et al. 1998, Costa et al. 2003, Georgiadis et al. 2003, Vanapalli et al. 2010).

Wet, dry, or submerged environments are usually taken into consideration while constructing pile foundations. It is now feasible to calculate the total shaft resistance of piles in unsaturated soils while considering matric suction by modifying the methods of Skempton (1959), Burland (1973), and Vijayvergiya and Fotch (1972). Numerous single-model pile tests were performed in a lab to evaluate how well these strategies functioned. In testing, pile shaft resistance was evaluated while it was buried in various saturation levels of statically compacted, unsaturated glacial till from Indian Head, Saskatchewan, Canada. The (α, β, and λ) and approaches support the modified principles that are often employed in pile design in the field of geotechnical engineering. Utilizing the saturated soil features and the SWCC, these approaches are functionally offered to estimate the variation of shaft capacity regarding matric suction. The proposed modified equations employ the conventional form of the (α, β, and λ) techniques for saturated soils

when the matric suction value is set to zero (Vinapalli et el.2012). The mechanics of unsaturated soil in the layers under the ground surface are shown in Figure 2-1.

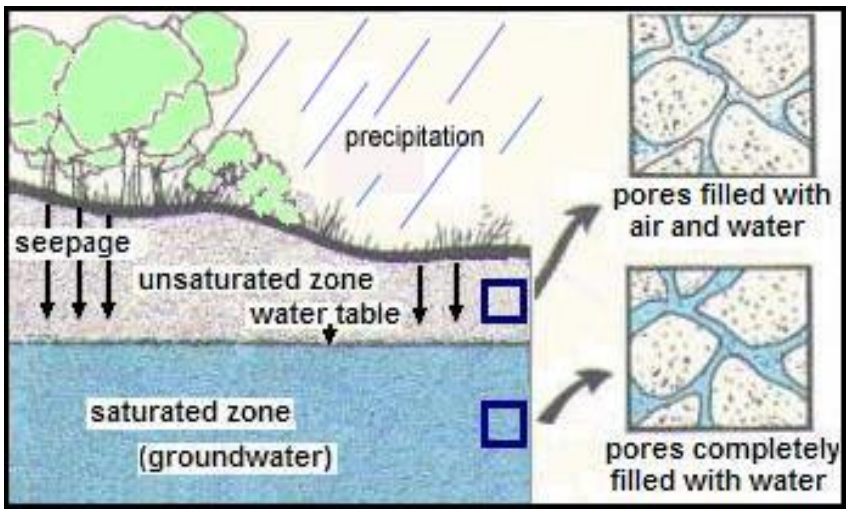

Figure 2-1 Effect of flux boundary conditions on unsaturated soil layers Source: NYSDEC

2.1 Unsaturated soil mechanics

The behavior of soils that are not saturated with water is the focus of the branch of soil mechanics known as unsaturated soil mechanics. This kind of soil is typically found in semi-arid and dry areas where there is not enough rainfall to completely soak the soil. Recently, there has been a lot of interest in the application of unsaturated soil mechanics to geotechnical engineering, notably in the design and analysis of structures constructed on unsaturated soils (Kristo et al., 2019). Because there is air in the soil pores, unsaturated soil behaves quite differently from saturated soil. When the saturation level drops, there is more air in the soil pores, which alters the soil's permeability, stiffness, and strength (Rahardjo et al., 2018). Unsaturated soils react differently to different loading scenarios, such as static and dynamic loads, due to variations in soil characteristics. Unsaturated soil mechanics revolves around the concept of the soil water characteristic curve. The relationship between the saturation level and the suction or matric potential of the soil is depicted graphically. The suction, which is brought on by the attraction of water molecules and soil particles, maintains water in soil pores in defiance of gravity's pull (Fredlund et al., 2012). The energy needed to draw water out of the soil is calculated using the matric potential. A tensiometer, which measures the soil's suction, is one piece of specialist equipment used in laboratory research to assess the water retention curve. The shear strength of unsaturated soils is the fundamental idea in unsaturated soil mechanics. How resistant a soil is to deforming under shear forces is determined by its shear strength. Suction and saturation levels have an impact on the shear strength in unsaturated soils. Due to the growing volume of air in the soil pores, when the saturation level drops, the shear strength also falls. The forces of attraction between soil particles and water molecules, which are heightened by suction, have an impact on shear strength. A shear strength envelope, which displays the shear strength at various suction levels, is a common visual representation of the connection between the shear strength and the suction (Vinapalli et el.2007). Unsaturated soils' permeability is a crucial factor in how they behave. The soil's ability to transmit water in the face of a pressure

gradient is determined by its permeability. The saturation level and the suction have an impact on the permeability of unsaturated soils. Because there is more air in the soil pores when saturation levels drop, permeability likewise declines. When the suction decreases the effective pore size and increases the tortuosity of the soil pores, permeability is also affected (Zhai et al., 2012). A permeability function, which is a mathematical formula that describes the change in permeability with respect to saturation, is frequently used to explain the relationship between permeability and the degree of saturation. The behavior of unsaturated soils may be influenced by the loading circumstances. The effective stress concept, which asserts that a soil's shear strength is a function of the effective stress, which is the difference between the total stress and the pore water pressure, governs the behavior of unsaturated soils under static loading conditions. Unsaturated soils react differently to dynamic loading circumstances due to variations in air pressure inside the soil pores, which can have an impact on the permeability and stiffness of the soil. Numerous studies have been conducted to examine the numerous dynamic characteristics that unsaturated soils exhibit under different loading circumstances (Fredlund and Rahardjo, 1993). Investigating how soils that are not entirely saturated with water behave is the essential subject of unsaturated soil mechanics. Various parameters, such as the level of saturation, suction, shear strength, permeability, and loading instances, might affect how unsaturated soils react.

2.2 Foundation design

The process of creating a construction plan for a building foundation is called foundation design. This highly sophisticated task is typically carried out by a structural engineer. The supporting structure that rests on the ground and sustains the rest of the building is called the foundation (Vinapalli et el.2012). The ground beneath the foundation, as well as its design and construction, must thus be thoroughly studied. Different types of building foundations exist. The majority of foundations may be constructed at a variety of depths, except slab-on-grade foundations, which are installed at ground level. Any foundation's depth may vary depending on several characteristics:

capabilities of soil: This establishes the maximum load (weight or force) that the soil can support.

soil type: Various soil types have various characteristics that may influence how well-suited they are to sustaining a foundation.

Frost depth: The frost depth or frost line, also known as the minimum depth for various types of foundations, is the depth at which the soil freezes during the coldest part of the year.

Groundwater table: The depth and type of foundation can both be restricted by a high groundwater table. A soil analysis usually includes information on groundwater height.

Minimum depth: In general, a foundation should be at least 18 inches deep to account for topsoil removal and differences in ground level, regardless of other circumstances.

The most common materials used to build foundations are poured concrete and masonry materials like concrete blocks and brick. Masonry materials are much more resistant to soil and moisture damage and have a high compressive strength compared to wood and metal. Brick foundations frequently rise above the ground to protect other building components from moisture and other damaging effects of earth contact (Morris et al. 1991). Rebar constructed of

metal or other materials is widely used to internally strengthen masonry foundations. Contractors routinely use hydraulic cement to seal off raceways and pipelines that enter masonry or concrete foundations.

One of the most important foundation components is the base, or subbase, which is composed of inorganic material and is positioned directly beneath the foundation. Typically, clay and submerged soil have low load-shaft capacities and cannot support the weight of a building. A dry, consistently thick material, like gravel or crushed stone, that offers the maximum shear resistance and shaft capacity is used to replace the removed soils. Moreover, unlike soil, which expands at high moisture levels, foundation materials help drain subterranean water (Costa et al. 2003, Georgiadis et al. 2003).

In order for the loads exerted on the foundations by the building to be dispersed evenly across the contact surface, the foundations must transmit the total of the dead load, live load, and wind load to the earth. The net loading capacity entering the shaft shouldn't be greater than its capacity (Vinapalli et el.2012). The projected building settling must be taken into consideration during foundation design to ensure that all movement is controlled and consistent and to prevent structural damage. It is crucial to research the overall design of the foundation, superstructure, and ground in order to identify potential building strategies that may be helpful (Pachkink et el.2013).

2.3 Soil water characteristic curve:

The soil water characteristic curve (SWCC), used in soil science, is an essential tool for understanding the relationship between soil water potential and soil water content. In agriculture, hydrology, and environmental science, it is crucial to comprehend this curve to understand how water travels through the soil and becomes available to plants (Zhai et al., 2019).

The soil water characteristic curve illustrates the relationship between a soil's water content and its water potential at equilibrium. The soil water potential is used to calculate the amount of energy required to remove water from the soil. It is comparable to the force that causes water to be drawn up out of the ground and used by a plant's roots or for another purpose. To display the SWCC, the soil water potential and water content are frequently shown on an x-y axis (Zhai et al., 2017).

The SWCC is influenced by a number of factors, including soil texture, structure, and organic matter concentration. The texture of the soil is determined by the proportions of sand, silt, and clay particles in that soil. High clay content soils frequently have steeper SWCCs than soils with low clay content, making it more difficult to remove water from the soil. Soil structure, SWCC as well since healthy soils often have bigger pores that facilitate water flow whereas poor soils typically have fewer holes that may hold water. The size and distribution of soil pores can be altered by an increase in organic matter content, which has an effect on the SWCC (Mercer et al., 2019).

The SWCC has several practical applications in soil studies. For example, it may be used to predict how much water a soil will be able to store at different soil water potentials. Since plants require water in the soil to grow and thrive, understanding how plants and water interact is crucial (Zhai et al., 2012). Additionally, irrigation systems tailored to the needs of a certain soil type may be designed using the SWCC. Additionally, the SWCC may help scientists and

engineers with the planning and assessment of soil stabilizing techniques, such as the use of compaction or soil additives.

The soil water characteristic curve is a crucial tool in soil science for comprehending the relationship between soil water potential and content. By studying the SWCC, scientists can predict how much water a soil can contain and how it would behave under certain conditions. Understanding how plants and water interact, creating irrigation systems, and evaluating soil stabilization techniques all require this understanding. Therefore, the SWCC is an essential tool in the toolbox of every soil scientist (Buranbayeva et al., 2012).

2.4 Foundation modelling and unsaturated soil analyses using plaxis:

Plaxis 3D is a finite element analysis application used to simulate the behavior of soil and buildings during foundation design. Retaining walls, deep foundations, and shallow foundations are just a few of the foundation types it may investigate. To represent the soil and the foundation design, engineers can utilize Plaxis 3D to build a 3D mesh of elements and nodes. The program may then model the behavior of the soil and foundation under various pressures, such as moments and vertical and horizontal loads. Along with other types of soil, Plaxis 3D can also study rock, sand, and clay. Additionally, it can replicate the soil's cohesion, internal friction angle, and stiffness. (Ayeman et al., 2006).

For the following reasons, Plaxis 3D is commonly utilized in foundation design:

Plaxis 3D may be used to evaluate the behavior of drilled shafts and piles as deep foundations. Design of shallow foundations: The settlement and shaft capacity of shallow foundations such as footings, rafts, and slabs can be investigated. During the design stage, Plaxis 3D may be used to examine the stability and deformation of retaining structures, such as walls and abutments (Mohammad Alkhaali et al., 2020).

By modelling the behavior of soil and structures, Plaxis 3D is a useful tool that may be utilized in foundation design to optimize the design of foundations and retaining structures.

The unsaturated soil analysis in Plaxis 3D simulates the behavior of soil with both air and water in its pores. This is distinct from saturated soil analysis, which involves completely submerging the soil in water. When investigating unsaturated soil, environmental factors such changes in temperature, humidity, or rainfall might have an impact on the soil's moisture content (Ayeman et al., 2006). The effects of soil suction and swelling/shrinking on soil behavior may also be simulated using Plaxis 3D. Modeling soil as a multi-phase material with separate solid, liquid, and gas phases is another option offered by Plaxis 3D. This makes it possible to examine the behavior of unsaturated soil more thoroughly while taking the influence of capillary forces and air pressure into consideration (Mohammad Rehan et al., 2022).

Geotechnical engineers may properly model and evaluate the behavior of unsaturated soils in a range of applications. Plaxis 3D's comprehensive suite of tools for evaluating unsaturated soils.

Chapter 3 Methodology

3.1 Applicable theory

Based on the fluctuation of shear strength with respect to matric suction, which can be calculated from SWCC and effective shear strength parameters, the Modified approach is used to calculate shaft capacity. Equation 1 presents a method for calculating shaft capacity based on the saturated soil mechanics theory. Equation 2 presents the improved approach for calculating shaft capacity based on the unsaturated soil mechanics theory. (Vinapalli et. el.2012)

$$Q_f = f_s A_s = \beta \sigma'_v \pi d L \quad (3.1)$$

$$Q_{f(us)} = [c'_a + \beta(\sigma'_z) + (u_a - u_w)(S^k)(tan\delta')]\, \pi d L \quad (3.2)$$

In equation (1) β= Burland-Bjerrum coefficient A_s= surface area of pile σ'_v= vertical effective stress at the mid of pile shaft L= length of the pile d= diameter of the pile

β Values varies from 0.30-0.60 for fine- and coarse-grained soils (Vanapalli et.al, 2012).

In equation (2) c'_a= adhesion component of cohesion for saturated condition δ'= effective angle of the interface along the soil/pile

The Modified α method is used to determine the variation of shaft capacity with respect to matric suction based on SWCC and undrained shear strength of soil (Vinapalli et el.2012).

$$Q_f = f_s \text{ x } A_s = \alpha c_u \pi d L \quad (3.3)$$

$$Q_{f(us)} = \alpha c_{u(sat)} [1 + \frac{(u_a - u_w)}{(\frac{p_a}{101.3})} sv/\mu]\, \pi d L \quad (3.4)$$

Pa= atmospheric pressure

ν , μ are fitting parameters, ν value depends on soil type. It takes 1 for coarse-grained soil, 2 for fine-grained soil.

$Luis$ Function of plasticity index Ip.

Modified λ method combines both previous methods, the total stress (undrained) and effective stress (drained) condition for calculating the shaft capacity of the pile foundation (Vinapalli et el.2012).

$$Q_f = \lambda\, (\sigma'_v + 2c_u)\ \pi d L \quad (3.5)$$

σ'_v= mean effective stress c_u= undrained shear strength along the pile length λ= functional capacity coefficient

λ is frictional capacity coefficient. λ Varies from 0.12-0.5 for pile penetration down to 70 meters (Vinapalli et el.2012).

$$Q_{f(us)} = \lambda\,[\sigma'_{v(avg)} + 2c_{u(sat)}(1 + \frac{(u_a - u_w)}{(\frac{p_a}{101.3})} sv/\,\mu)]\,\pi dL \quad (3.6)$$

Numerous formulae have been presented to assess the potential of soil moisture due to the great mechanical variability of soils and the difficulty of experimentally determining the whole SWCC. Fredlund and Xing (1994) improved the equation by adding independent parameters a, n, m, and s as a result of their collaborative research on discovering the optimal approach for fitting SWCC. (Fredlund and Xing, 1994).

$$\theta = \left[1 - \frac{ln\left(1+\frac{\psi}{C_r}\right)}{ln\left(1+\frac{10^6}{C_r}\right)}\right]\left\{\frac{\theta_s}{\left\{ln\left[e+\frac{\psi}{a}\right]^n\right\}^m}\right\} \quad (3.7)$$

Where ψ = matric suction; e = base of natural logarithm; a = fitting parameter related to the air entry value of the soil; n = fitting parameter related to the maximum slope of the curve; m = fitting parameter related to the curvature of the slope; Cr = correction factor.

3.1.2 Research method

This study includes two different types of analyses: analytic calculations using the six methods (α, β, and λ and modified α, β, and λ), taking into account various groundwater table depths, and numerical calculations using plaxis 3D to analyze the impact of rainfall on the shaft capacity of pile foundations concerning matric suction changes.

In the analytical calculation for course-grained soil fifteen sets of calculations were done to measure the shaft capacity of the foundation in state of saturated for 10m, 8m, 6m, 4m, and 2m depth of foundation using α, β, and λ methods and fifteen sets of calculation was performed to calculate the shaft capacity of pile foundation in state of unsaturated for 10m, 8m, 6m, 4m, and 2m depth of foundation using modified α, β, and λ method. For fine-grained soil, the same amount of calculation sets was performed. The result is calculated by comparing the two standard calculating techniques.

To evaluate the impact of rainfall on the shaft capacity of pile foundations, analytical calculations were made utilizing the results of numerical computations performed using plaxis. For this objective, fifteen sets of analytical calculations using the modified, and technique were made for soil with a coarse grain, and fifteen sets were made for soil with a fine grain.

Because of the current state of buildings in Astana, Kazakhstan, and because of the city's heavy summer rainfall, the study specifically examines how rainfall affects the qualities of unsaturated soil there. According to Astana geological distribution, the groundwater table's maximum depth is 10 meters, while the average depth is between 2 and 10 meters (Zhussupbekov et al. (2012).

3.2. Laboratory testing

Laboratory testing was conducted to obtain unsaturated soil properties for foundation design. For this thesis work laboratory testing was on two types of soils, course-grained soil (sand) and fine-grained soil (kaolin).

3.2.1 Soil-water characteristic curve (SWCC)

The soil-water characteristic curve cannot be obtained without sophisticated laboratory testing. Unsaturated soil's behavior is heavily reliant on SWCC (Satyanaga et al., 2017). To produce SWCC, HYPROP testing equipment was employed. Hyprop is seen in Figure 3-1. The natural evaporation process that occurs during testing is a part of the mechanism for employing Hyprop. The soil water characteristic curve (SWCC) is widely used to describe soil physical behavior, irrigation, drainage, and nutrient transfer. However, SWCC measurement is typically time-consuming, labor-intensive, and inaccurate. To acquire an accurate SWCC, HYPROP is employed. The steps covered in this technique article include collecting soil samples, utilizing the HYPROP refill unit, and degassing water before degassing tension tubes, among other things. Advice is provided on how to use the tools more skillfully to obtain all four phases of the ideal measurement curve. (Satyanaga et al., 2020).

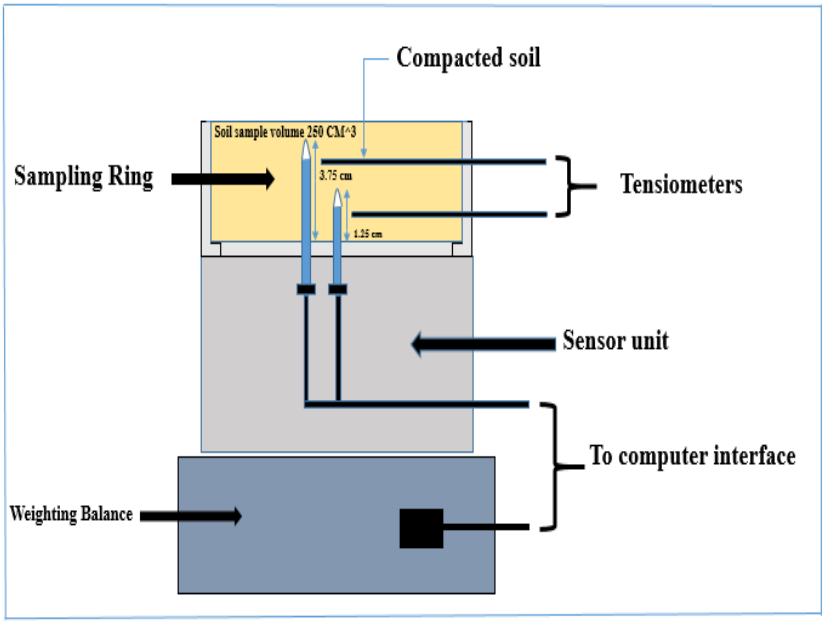

Figure 3-1 Cross section Hyprop

For SWCC up to 100kPa soil suction, HYPROP is employed. Two tensiometers in HYPROP have varying depths. This tool is used to measure SWCC between 500 kPa and 200,000 kPa. (Satyanaga et al., 2017). Figure 3-2 illustrates how to create a soil water characteristic curve using hyprop.

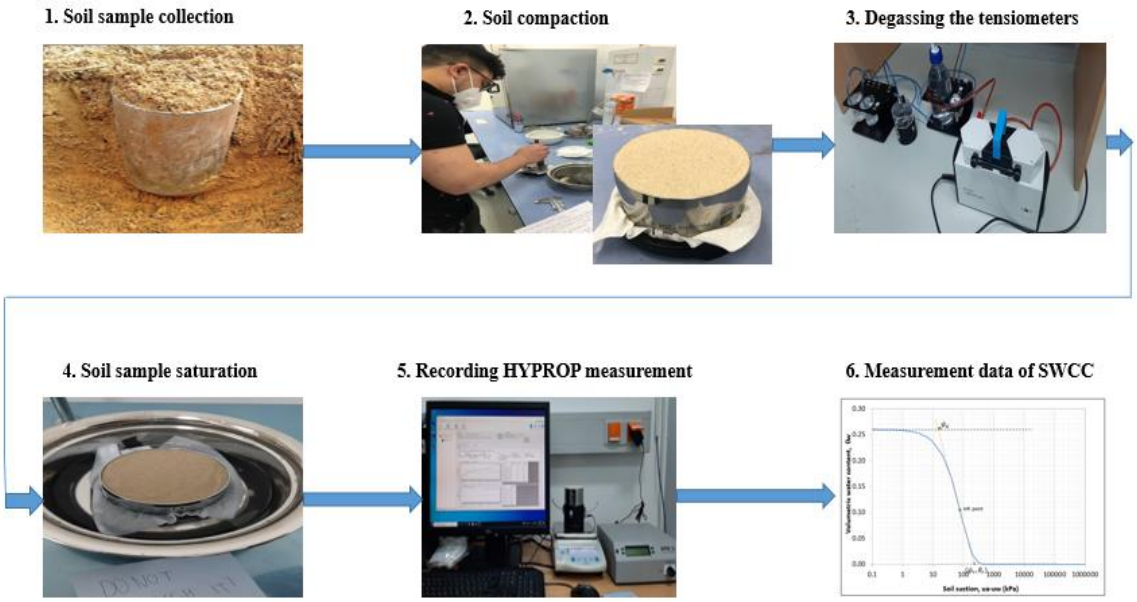

Figure 3-2 Measurement of soil water characteristic curve using Hyprop

3.2.2 Grain size distribution:

For soil categorization, analyses of grain size distribution using sieve and hydrometer tests were carried out. Particle size distribution is the range of sizes of particles in a particular substance and is frequently expressed as a percentage of the total number or mass of particles in each size range. This understanding is essential in a range of areas, including material science, chemistry, and environmental engineering, because the size of particles may influence properties like reactivity, solubility, and filtration. Particle size distributions may be determined by a variety of methods. includes hydrometer studies ASTM D7928-12e1 shown in Figure 3-4 and sieve grain-size analyses ASTM D422-63 shown in Figure 3-3, all of which were employed for the current study effort on course- and fine-grained soils (Sand and Kaolin), respectively.

Using a hydrometer to examine the soil, Stokes' law is used to calculate the size of soil particles based on how rapidly they detach fa from a liquid suspension. The results of the test demonstrate how the grain size distribution varies for soil finer t n No. the 200 (75 m) sieve. They do, however, provide a full gradation profile of soils that includes coarser components when used in conjunction with a sieve inspection. The grain size figure in fiFigure-3 and hydrometer Figure 3-4 are shown.

Figure 3-3 Grain-Size Analysis

Figure 3-4 Hydrometer analysis

3.2.3 Specific gravity analysis:

Specific gravity is the ratio of a substance's density to a reference density, frequently deionized water. (SG). It is, in other words, the ratio of the substance's mass to a reference mass for a given volume at ambient temperature. Specific gravity is a dimensionless number that is impacted by pressure and temperature since it is a ratio of densities. Therefore, the sample and reference densities must be calculated at the same pressure and temperature. The ASTM D854-06 specific gravity measuring device is shown in Figure 3-5.

Figure 3-5 Gravity Test

3.2.4 Index properties by Atterberg limit:

The liquid and plastic limits of soil are referred to as the Atterberg limits. International standards for soil identification, categorization, and strength correlation employ these two limitations. Fine-grained soil that contains clay minerals may be formed in the presence of moderate rainfall without dissolving. The water that has been adsorbed around the clay particles is what gives them their cohesion. Soil behaves more like a solid at extremely low moisture levels,

whereas water may flow through the soil like a liquid at very high moisture levels. The shrinkage limit is the percentage of moisture content at which solid changes into a semi-solid condition. (SL). The plastic limit (PL) is the moisture level at the boundary between semi-solid and plastic states, while the liquid limit is the moisture level at the boundary between liquid and plastic states. (LL). Atterberg limits are another name for these parameters. It is possible to express a soil's relative consistency or fluidity index using its liquid and plastic limits as well as its water content. Its activity number may be calculated using the plasticity index and the fraction of particles smaller than 2 m. The Atterberg limit shows Figure 3-6 was used for the classification of fine-grained soil based on -ASTM, D4318-10

Figure 3-6 Atterberg test equipment

3.2.5 Saturated Permeability (k_s):

Saturated permeability (ks) is calculated using a constant head, as shown in Figure 3-7 for coarse-grained soil, and a falling head, as shown in Figure 3-8 for fine-grained soil. In the constant head permeability test, water is forced through a cylindrical soil sample column while the pressure difference remains constant. The experiment is conducted in a permeameter, commonly known as a permeability cell. The soil sample is fashioned like a cylinder and has a big enough diameter to correctly reflect the soil under study. Common test cells for common sands are generally 75 mm in diameter and 260 mm in height between perforated panels. The testing device features an output reservoir and an adjustable constant head reservoir for maintaining a constant head during the test. De-aired, constant-temperature water is utilized for testing. A loading piston is another feature of the permeability cell that may be utilized to deliver continuous axial stress to the test material. However, the soil sample is wet before the flow measurements begin. Water flow through the soil column is measured periodically throughout the test.

For fine-grained soils with intermediate and low permeability, such as silts and clays, with permeability in the range of 1x10-5 to 1x10-9, the falling head permeability test is utilized. An undisturbed sample can be used for this testing

technique. Both an undisturbed sample in a sampling tube and a sample in an oedometer consolidation cell may be analyzed using the falling head theory.

Using a rigid-wall, compaction-mold permeameter, this test method allows for the measurement of the hydraulic conductivity of laboratory-compacted materials. It can be used with compacted specimens that have a hydraulic conductivity of less than or equal to 1 105 m/s.

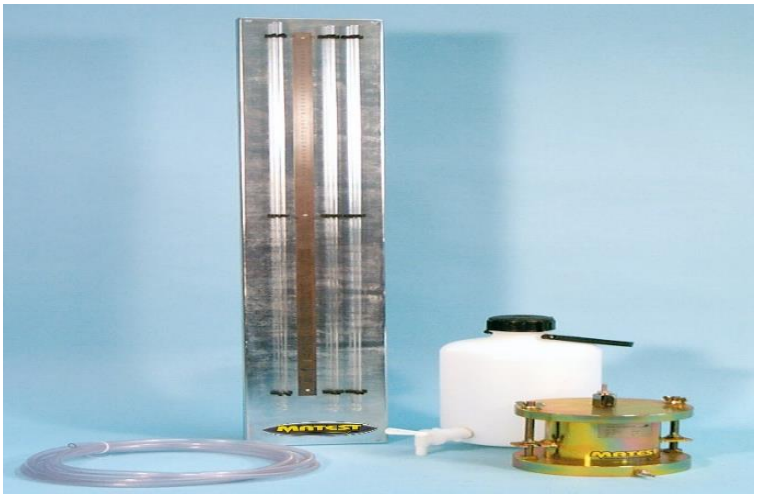

Figure 3-7 Falling head permeability test

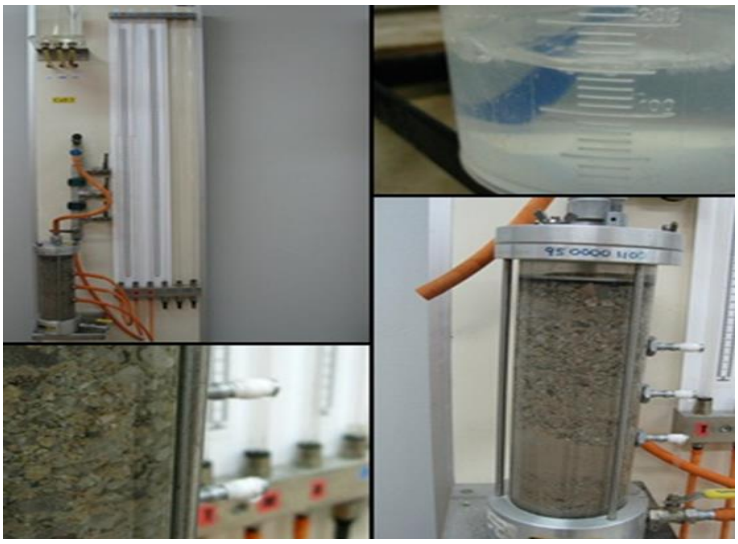

Figure 3-8 Constant head permeability test

3.2.6 Shear strength test using Triaxial

The CU and CD triaxial test was used to obtain the soil's shear strength parameters (c', Φ') for efficient stress analysis for fine and course-grained soil. CU and CD tests may be used to look at the development of pore pressure inside the soil mass as well as the soil's reaction to stress and strain. In the CU and CD tests, the material is consolidated by permitting drainage while confining pressure (c) is applied. This is ensured by watching to make sure that after a specific length of time under the applied pressure, there are no more leaks. Consolidation is complete, and the specimen is now ready to be sheared. A triaxial test is often used in labs to assess the strength and stress-strain properties of soil or rock specimens under certain loading circumstances.

A triaxial test is performed on a cylindrical soil specimen that is contained in a cell by a rubber membrane. The specimen is then put to a variety of axial and confining pressures while the deformation and stress responses are measured. The test can be carried out in either drained or undrained conditions, depending on the intended usage.

The three primary stresses acting on the test specimen are the two lateral stresses, which are applied parallel to the axis, and the axial stress, which is applied perpendicular to the specimen's axis. Multiple loading conditions may be given to the specimen during a triaxial test due to the independent management of these three stresses.

The findings of a triaxial test may be used to determine crucial traits of the soil or rock specimen, including shear strength, Young's modulus, Poisson's ratio, and the stress-strain relationship under various loading scenarios. These features are crucial for building and foundation design, slope and retaining wall analysis, and stability evaluation of naturally existing slopes and excavations. The ASTM D4767-11 served as the foundation for the shear strength triaxial test seen in Figure 3-9

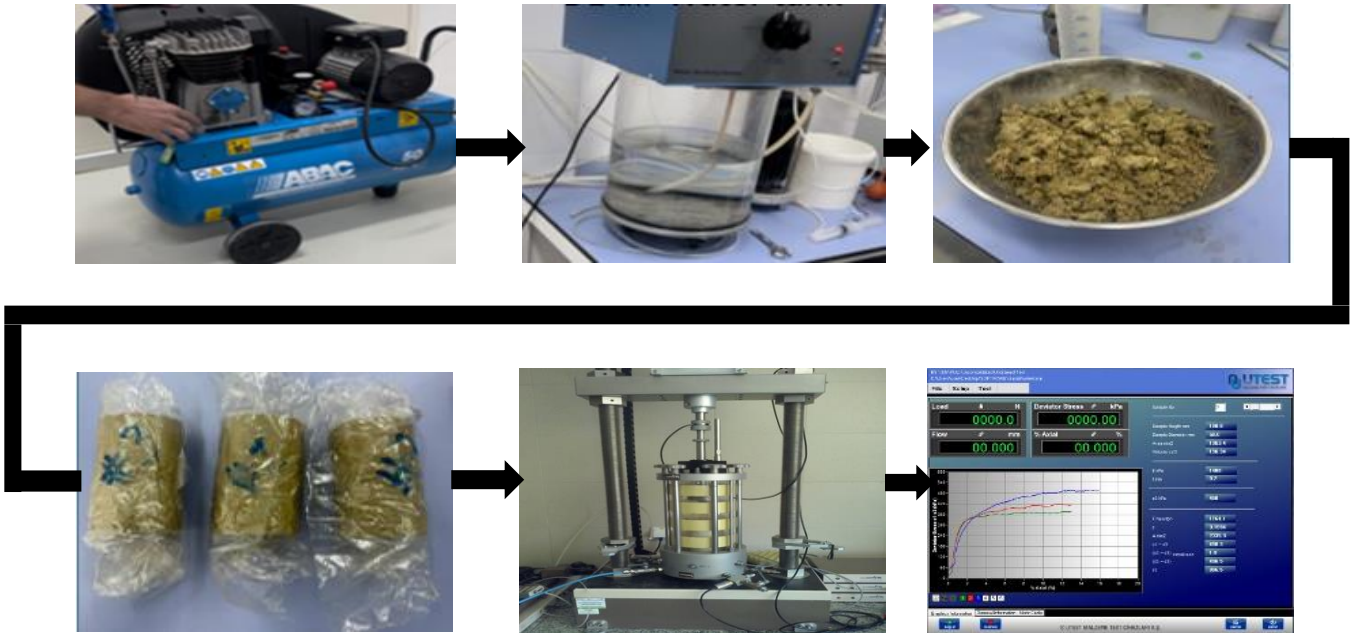

Figure 3-9 Triaxial test

3.3 Numerical analyses using Plaxis 3D:

Using the finite element approach, users of the powerful geotechnical analysis tool PLAXIS 3D may simulate complicated soil and rock dynamics. (FEM). The program is often used for deep excavations, foundation systems, and tunnel analysis and design.

The basic steps for creating a 3D model in PLAXIS 3D are as follows:

1. Make a new undertaking: the analysis's 10-noded elements, full model type, the unit is the meter and 12-by-12-meter border area. according to Figure3-10.

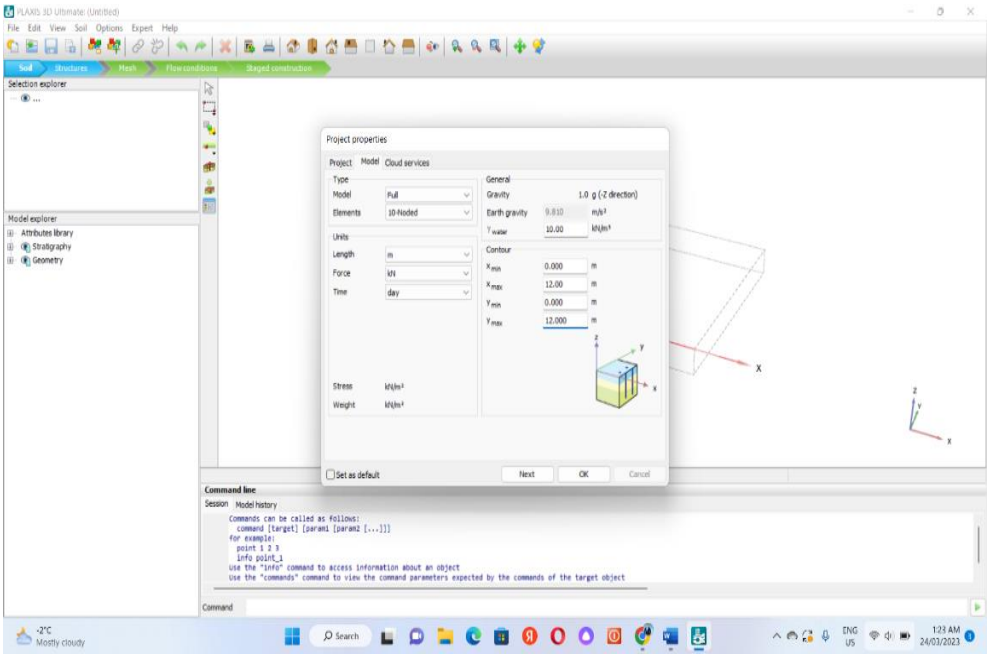

Figure 3-10 Choosing project properties in Plaxis 3D

2. Construct the geometry: This stage creates the borehole where the depth of soil layers can be keyed in and also the depth of the f groundwater table. Shown in Figure 3-11.

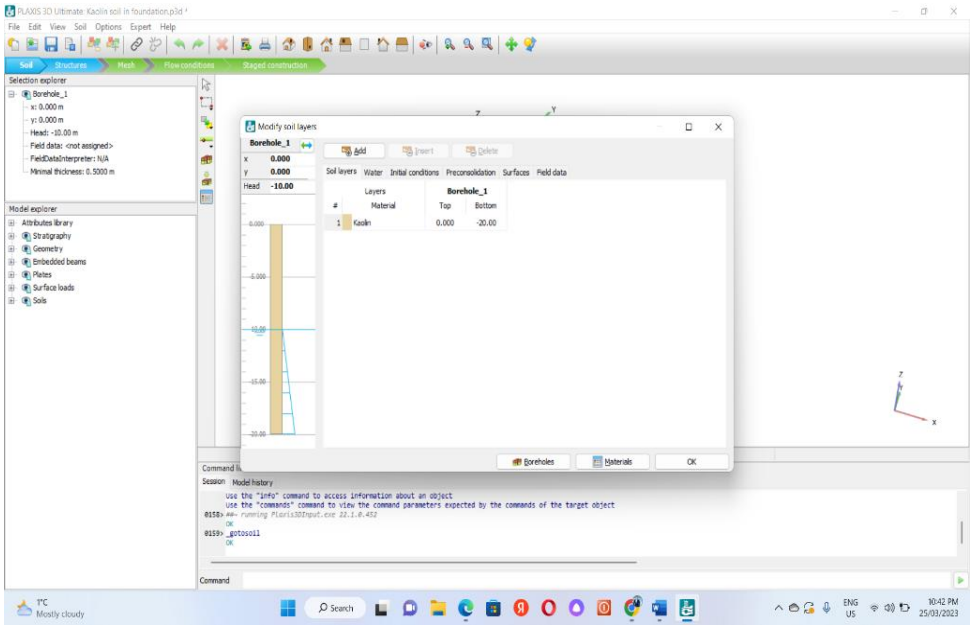

Figure 3-11 Creating a borehole in Plaxis 3D

3. Give details about the materials: Describe the elements of the building and the soil in the model, respectively. This category may contain characteristics like density, stiffness, and strength. According to the triaxial test, modules of elasticity are 430kN/m3, soil cohesion is zero, friction angle is 45 degrees, unite soil weight is 16kN/m3, saturated unit weight is 20kN/m3, and the soil model chosen for pile modeling in the sand Mohr-Coulomb. Similar results are obtained for pile modeling using plaxis in kaolin, where the soil model is mohr coulomb, the drainage type is drained, the unsaturated unite weight of the soil is 18.3 kN/m3, the saturated unite weight of the soil is 20.83 kN/m3, the modules of elasticity are 15.76 kN/m3, the soil cohesion is 18 kPa, and the friction angle is 23 degrees. Figure 3-12a depicts the general characteristics of the soil, whereas Figure 3-12b depicts the mechanical characteristics of the soil.

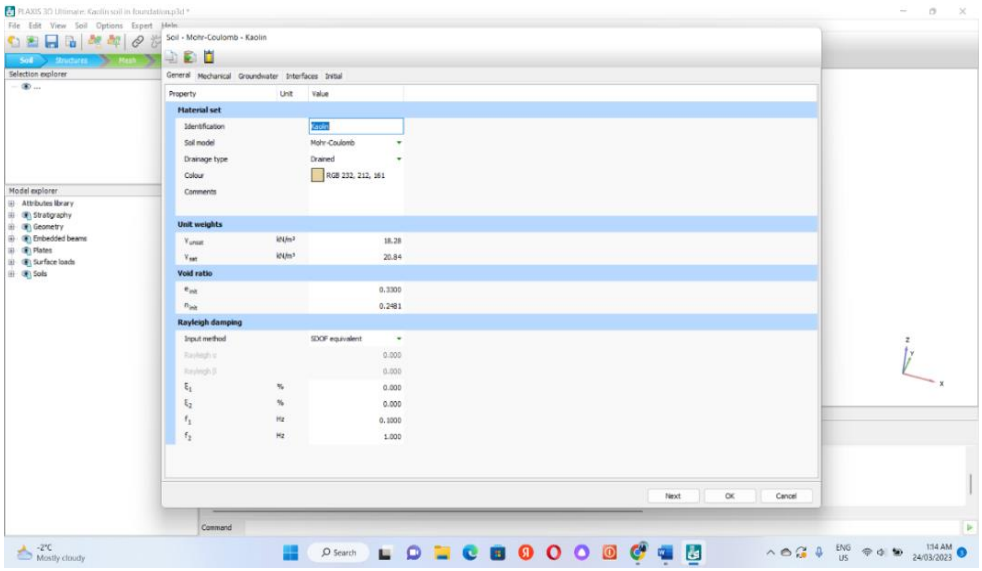

Figure 3-12a General properties of soil for foundation modelling using Plaxis 3D

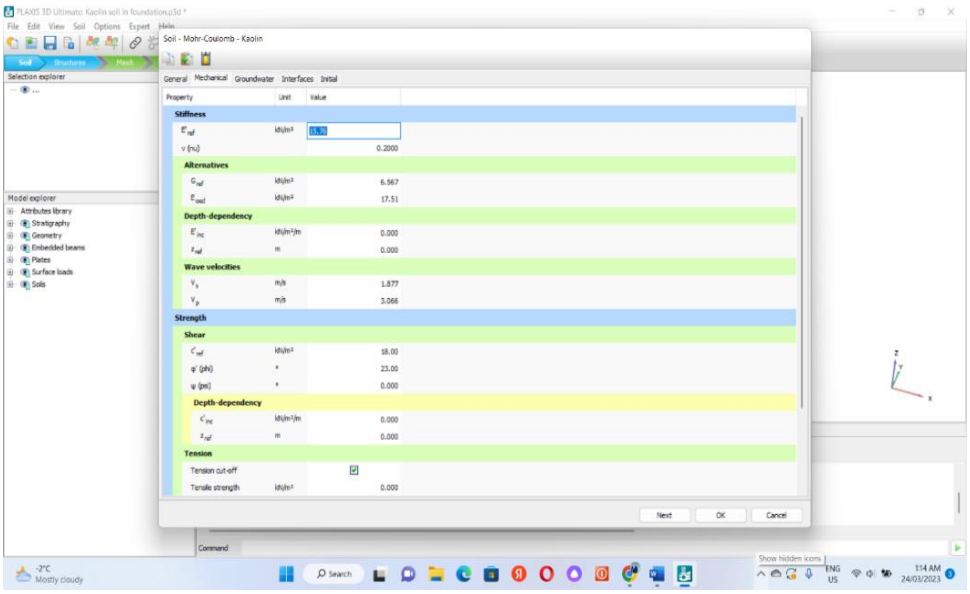

Figure 3-12b Mechanical properties of soil for foundation modeling using Plaxis 3D

4. SWCC and permeability graphs are created using the groundwater option in the soil modeling section. This option allows users to enter the soil suction, permeability, and degree of saturation values in a table, and then generate SWCC and permeability graphs. shown in Figure 3-13.

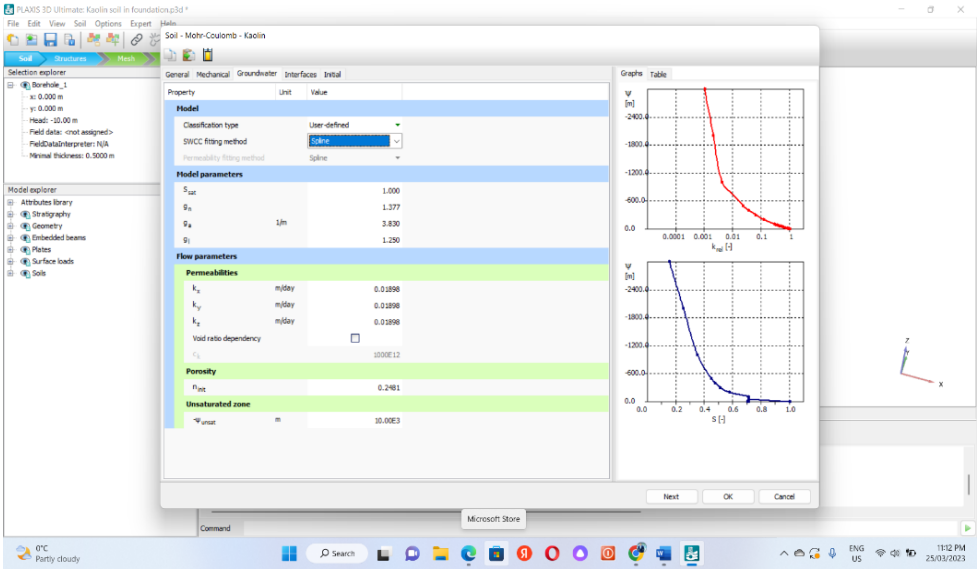

Figure 3-13 Creating SWCC and permeability graphs using Plaxis 3D

5. Create a mesh of the model to discretize the geometry and facilitate the use of finite element analysis.

The mesh size for this modeling is chosen as fine. The minimum element dimensions the of mesh is 0.918 mm. shown in Figure 3-14.

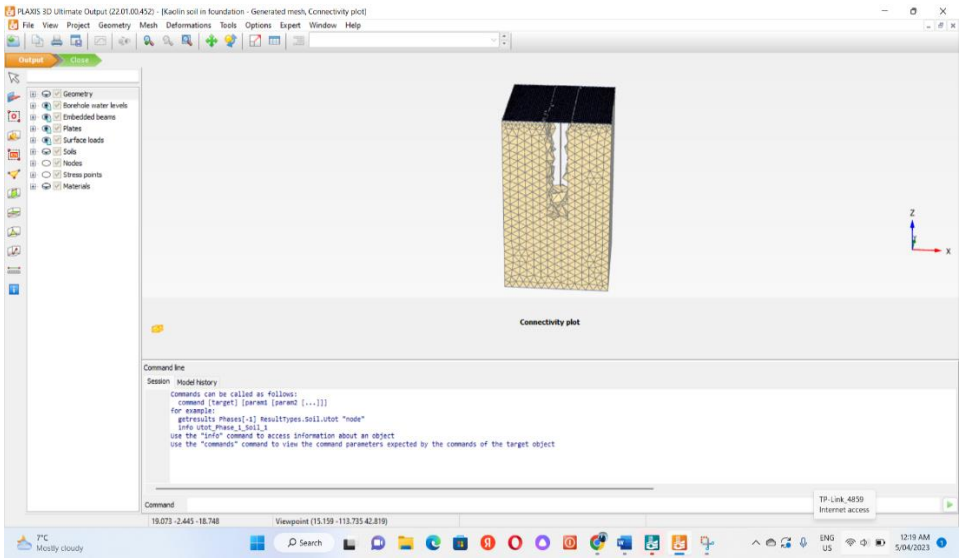

Figure 3-14 Creating a mesh in Plaxis 3D

6. Precipitation addition: 12 days of rain is followed by a 12-day dry spell. In Astana, Kazakhstan, it rains at a rate of 20mm per day (0.02m per day). The largest amount of precipitation is 12 days at 20mm per day. (Chepelianskaia et al., 2022). The volume of rainfall as well as the time interval of rainfall can be added in the stage creation step of modeling using Plaxis. As illustrated in figure 3Figurehe discharge function, where the duration and the amount of precipitation may be added, can be modified in the attribute library's flow function.

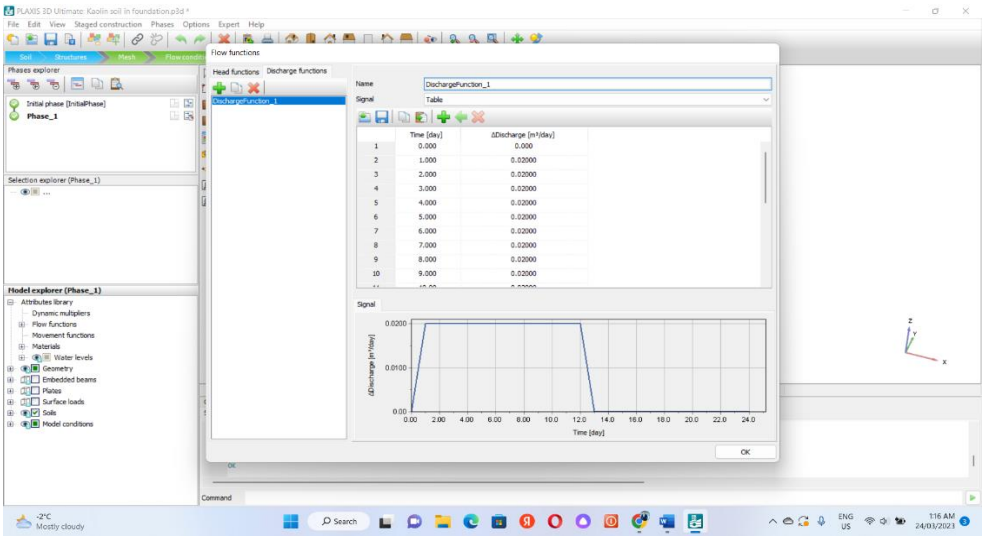

Figure 3-15 Precipitation in foundation modeling using Plaxis 3D

Figure 3-16 illustrates the result of 3-D modeling of the pile foundation using pPlaxis3-D.

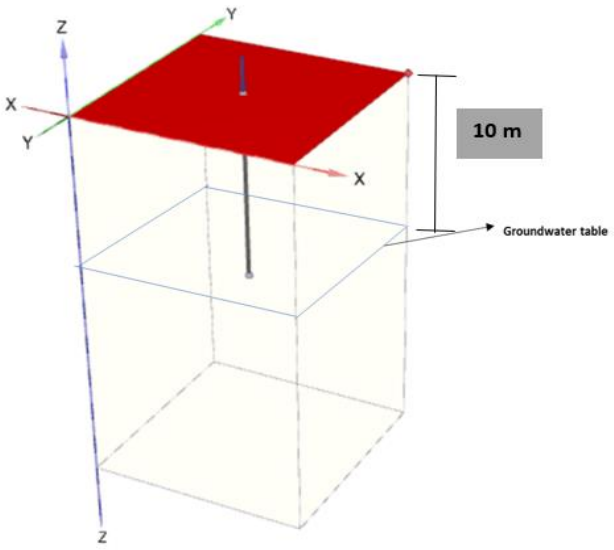

Figure 3-16 Foundation modeling using Plaxis 3D

3.3.1 Mathematical equation used in modelling pile in plaxis:

Richard equation 3.8 is used for water infiltration calculation in plaxis.

$$-n[s/k_w-\partial s/\partial p_w]\ \partial p_w/\partial t+\nabla^{T[k}{}_{rel}/\rho_w g*k^{sat}(\partial p_{w+}\ \rho_w g)]=0 \qquad (3.8)$$

The above equation is a form of the well-known Richards equation which describes saturated-unsaturated groundwater flow. The Richards equation has the following form (e.g. Dogan & Motz (2005)):

$$\{\partial/\partial x[k_x(h)\ \partial h/\partial x]+\ \partial/\partial y[k_y(h)\ \partial h/\partial y]+\ \partial/\partial y[k_z(h)\ (\partial h/\partial z+1)]\}=[c(h)+s.s_s]\ \partial h/\partial t \qquad (3.9)$$

where Kx , Ky and Kz are permeability coefficients in x, y and z directions, respectively. $C(h)=(\partial\theta/\partial h)$ is the specific moisture capacity (L^{-1}) and Ss is the specific storage (L^{-1}). The specific storage Ss is a material property that can be expressed as:

$$s_{s=}\ \rho_w g[1-n/k_s+n/k_w] \qquad (3.10)$$

The compressibility of soil particles can be neglected, therefore:

$$s_{s=}n\ \rho_w g/kw \qquad (3.11)$$

The term C(h) in the Richards equation can be expanded as:

$$C(h)=\ \partial\theta/\partial h=\partial/\partial h(nS)=n\ \partial s/\partial h \qquad (3.12)$$

By substituting equations (3.12) and (3.13) in the Richards equation (Eq. 3.9) and changing from a head-based equation ta o pore water pressure-based equation, equation (3.8) is obtained.

3.4 Geotechnical database

3.4.1. Development of a geotechnical database for Astana city

Astana was examined first since it has been the subject of substantial engineering-geological mapping studies based on field and laboratory research. based on the study of Zhussupbekov et. Al. (2012) used the sites of existing boreholes to assess the mechanical and physical characteristics of the soil. (Buranbayeva et al., 2012). In line with Shaldykova et. According to Al. (2020), the three zones makeup up Astana's area were built based on the soil profile. The mechanical and physical properties of coarse-grained and fine-grained soils, which are described in Tables 3-1 to Table 3-3, must be individually summarized as the aim of this research is to develop a soil-water characteristic curve for diverse soil types.

Table 3-1 Engineering properties of coarse-grained soil for Astana city

Zone	Soil Type	Cohesion, ***c***, kPa	Elastic Modulus, E Mpa
2	Silty medium gravel	1.0	29.0
2	Sandstone	2.0	32.0
3	Medium dense sand	2.0	17.0
3	Gravelly sand	1.0	12.0
3	Sandy gravel	2.0	25.5

Table 3-2 Index properties of fine-grained soil for Astana city

Zone	Soil Type	Moisture content, w (%)	Liquid limit, LL (%)	Plastic Limit, PL (%)
1	Loam	16.1	26.0	15.0
1	Clay	31.1	60.0	35.0
1	Clay	33.0	60.0	41.0
1	Clay	31.4	70.0	44.0
2	Sandy loam	20.9	24.0	15.0
2	Clay	28.7	63.0	36.0
2	Clay	28.0	68.0	36.0
2	Clay	31.1	60.0	35.0
2	Clay	33.6	71.0	41.0

Table 3-3 Engineering properties of fine-grained soil for Astana city

Zone	Soil Type	Elastic Modulus, E Mpa	Cohesion, ***c***, kPa	Friction angle, ϕ (º)
1	Loam	7.9	-	-
1	Clay	9.3	-	-
1	Clay	11.9	53.3	17.5
1	Clay	9.1	45.3	20.6
2	Sandy loam	7.2	18.2	-
2	Clay	6.9	45.0	10.8
2	Clay	7.2	45.0	10.8
2	Clay	8.8	37.3	20.6
2	Clay	-	50.0	14.0

Chapter 4 Results from laboratory testing, analytical calculations, and numerical analyses

4.1 Analyses of soil properties in Astana:

4.1.1 Regression analysis of soil properties:

The link between liquid limit and cohesion may be shown through an investigation of the soil in Astana, which will demonstrate the cohesiveness scale. Therefore, a high liquid limit value denotes a high level of cohesiveness. Figure 4-1 shows that the R-square (R2) is close to 1, demonstrating a clear connection between cohesiveness and liquid limit. A graph cannot be made since there is no information on the liquid limit for coarse-grained soil. The next step is to determine how friction angle and elastic modulus relate to one another.

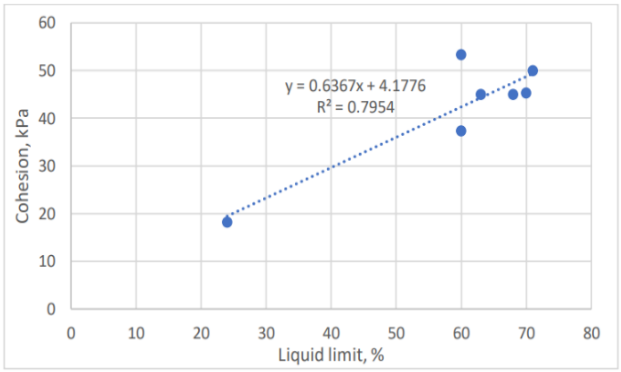

Figure 4-1 Cohesion vs. Liquid limit for fine-grained soils of Astana

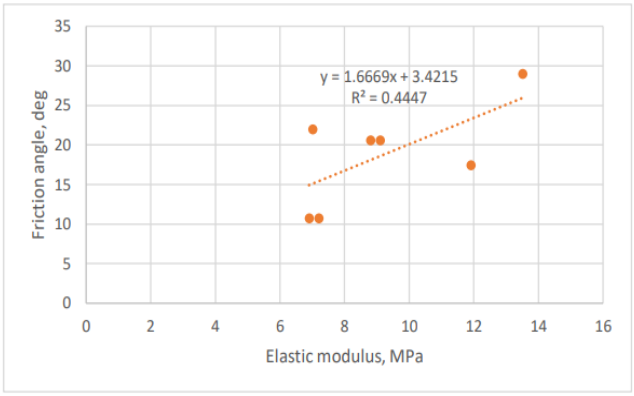

Figure 4-2 Friction angle vs Elastic modulus for fine-grained soils of Astana

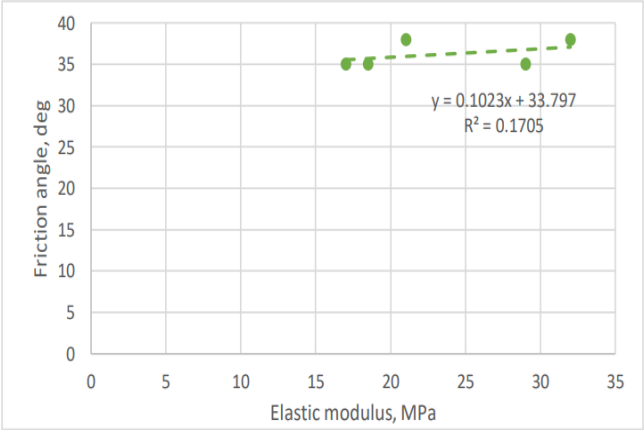

Figure 4-3 Friction angle vs Elastic modulus for coarse-grained soils of Astana

4.1.2 Soil Classification

To plot the soil-water characteristic curve, the soil categories must be identified. The soil classification for the study regions was created and is shown in Tables 4-1 through 4-5 using the Unified Soil Classification System and Casagrande's plasticity chart.

The categorization of soils for other regions was carried out based on the examination of the available soil attributes and soil types that were described in the preceding sections since only the Atterberg limits are available for soils in Astana.

Due to a lack of soil data, it is not possible to divide Western Kazakhstan's fine-grained soils into several soil categories. As a result, this section gets skipped.

Table 4-1 Soil classification of coarse-grained soil for Astana city

Zone	Soil classification (Symbol)	Soil classification (Group name)	Elastic Modulus, E Mpa	Friction angle, ϕ (°)
2	GM	Silty gravel	29.0	35
2	GW	Well-graded gravel	32.0	38
3	SW	Well-graded sand	17.0	35
3	SP	Poorly-graded sand	12.0	38
3	GP	Poorly-graded gravel	18.5	35

Table 4-2 Soil classification of fine-grained soil for Astana city

Zone	Soil classification (Symbol)	Soil classification (Group name)	Liquid limit, LL (%)	Plastic Limit, PL (%)
1	CL	Silty clay	26.0	15.0
1	MH	Silt with high plasticity	60.0	35.0
1	MH	Elastic silt	60.0	41.0
1	MH	Elastic silt	70.0	44.0
2	CL	Clay with low plasticity	24.0	15.0
2	MH	Elastic silt	63.0	36.0
2	MH	Elastic silt	68.0	36.0
2	MH	Elastic silt	60.0	35.0
2	MH	Elastic silt	71.0	41.0

Table 4-3 Index properties of Sand and Kaolin

Index properties	Kaolin	Sand
Specific gravity Gs	2.69	2.64
Liquid Limit, LL (%)	66.3	
Plastic Limit, PL (%)	41.7	
Plasticity Index (%)	24.6	
Void Ratio, e	0.33	0.71
Dry Density. (Mg/ m^3)	1.45	1.5
Water Content, W (%)	28.5	25.9
Soil Classification according to USCS	MH	SW

4.2 Results from experimental works carried out in this study

4.2.1 Particle size distribution curve:

Table 4-4– Index properties of course-grained soil (sand) and fine-grained soil (Kaolin)

Soil Type	**Sand SW**	**Kaolin** MH
Specific gravity, Gs	**2.64**	**2.69**
Liquid Limit, LL (%)		**66.3**
Plastic Limit, PL (%)		**41.7**
Plasticity Index, PI (%)		**24.6**
Void Ratio, e	**0.71**	**0.33**
Dry density, ρd (Mg/m^3)	**1.5**	**1.45**
Water content, w (%)	**25.9**	**28.5**
D_{60} (mm)	**2.36**	
D_{30} (mm)	**0.7**	
D_{10} (mm)	**0.1**	
Coefficient of uniformity, C_U	**23.6**	
Coefficient of curvature, C_C	**2.07**	

The result of the sieve analysis for creating particle size distribution of sand is shown the figure 4-4. And the result of particle size distribution of Kaolin using hydrometer analyses is shown in Figure 4-5.

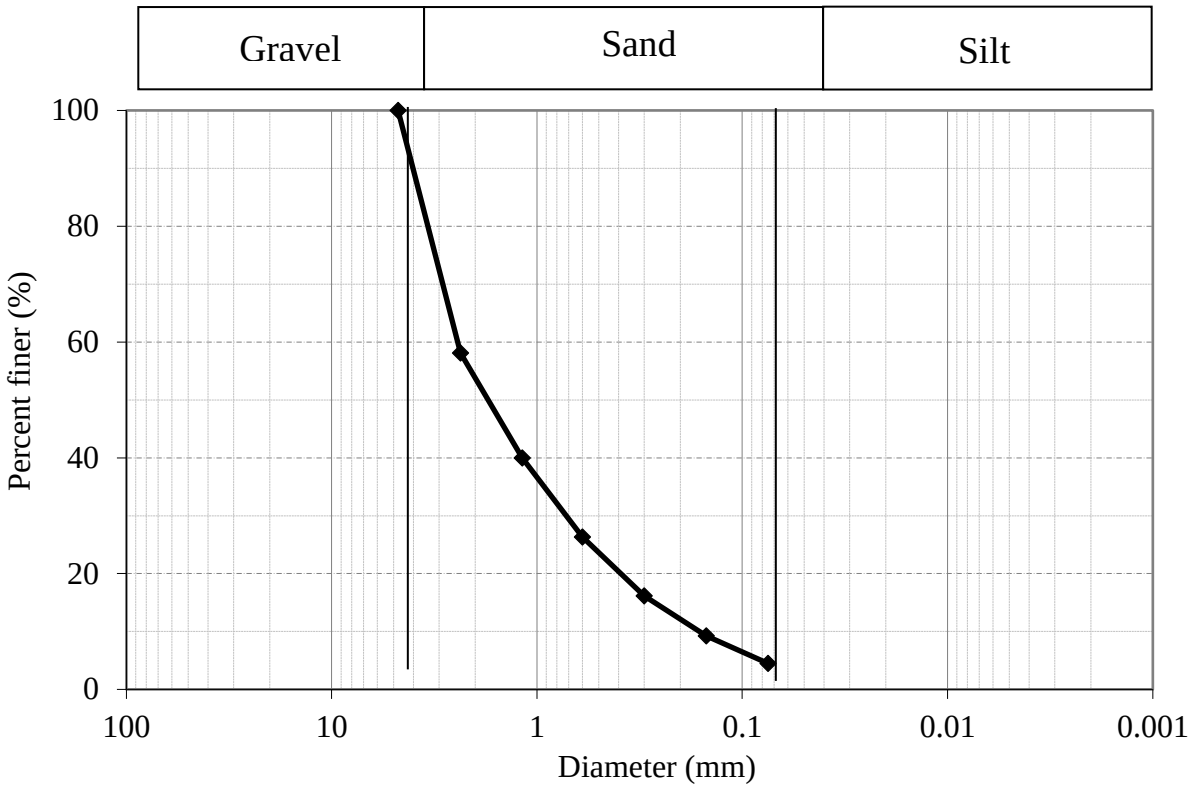

Figure 4-4 Particle size distribution of Sand

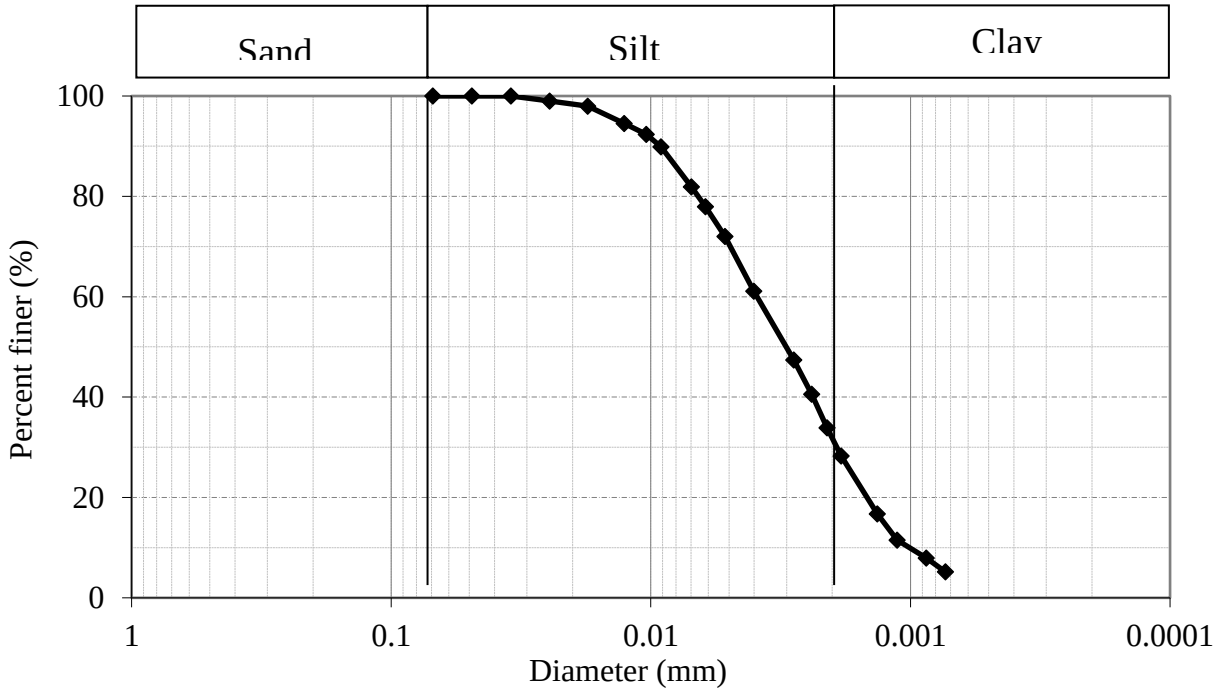

Figure 4-5 Particle size distribution of Kaolin

4.2.2 Permeability of Soil:

Figure 4-6 shows the results of measuring the saturated permeability of sand using the constant head test. The Kaolin falling head test is used to determine the permeability of fine-grained soil, and the results are displayed in Figure 4-7.

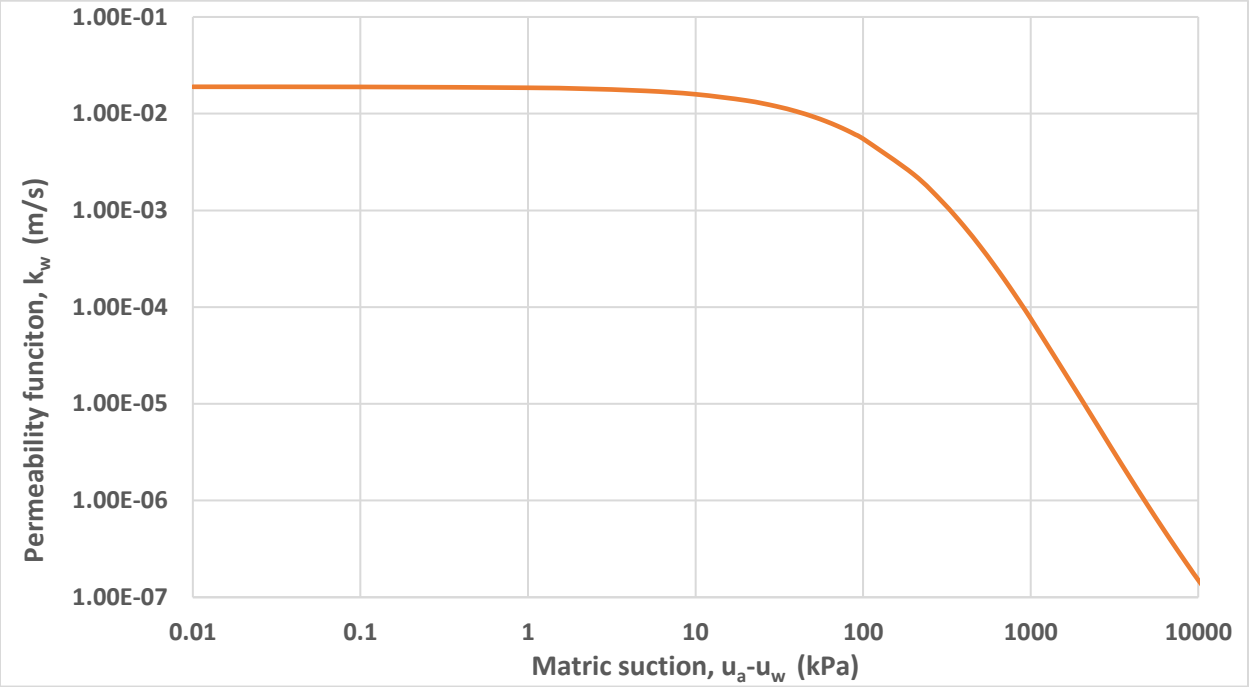

Figure 4-6. Permeability of sand

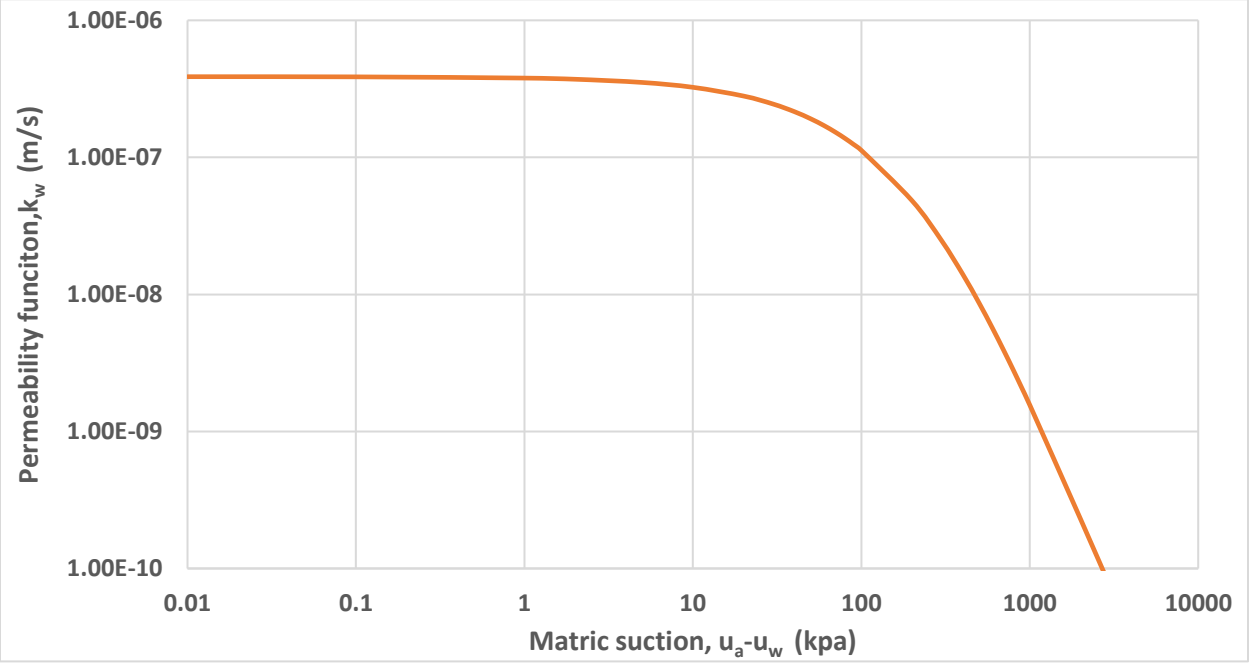

Figure 4-7 Permeability of kaolin

Figures 4-8 and 4-9, which were produced using the Hyprop testing tool, depict the soil water characteristic curve (SWCC) of sandy soil and the SWCC of kaolin, respectively. For this curve, the best-fitting equation was employed (Fredlund and Xing, 1994).

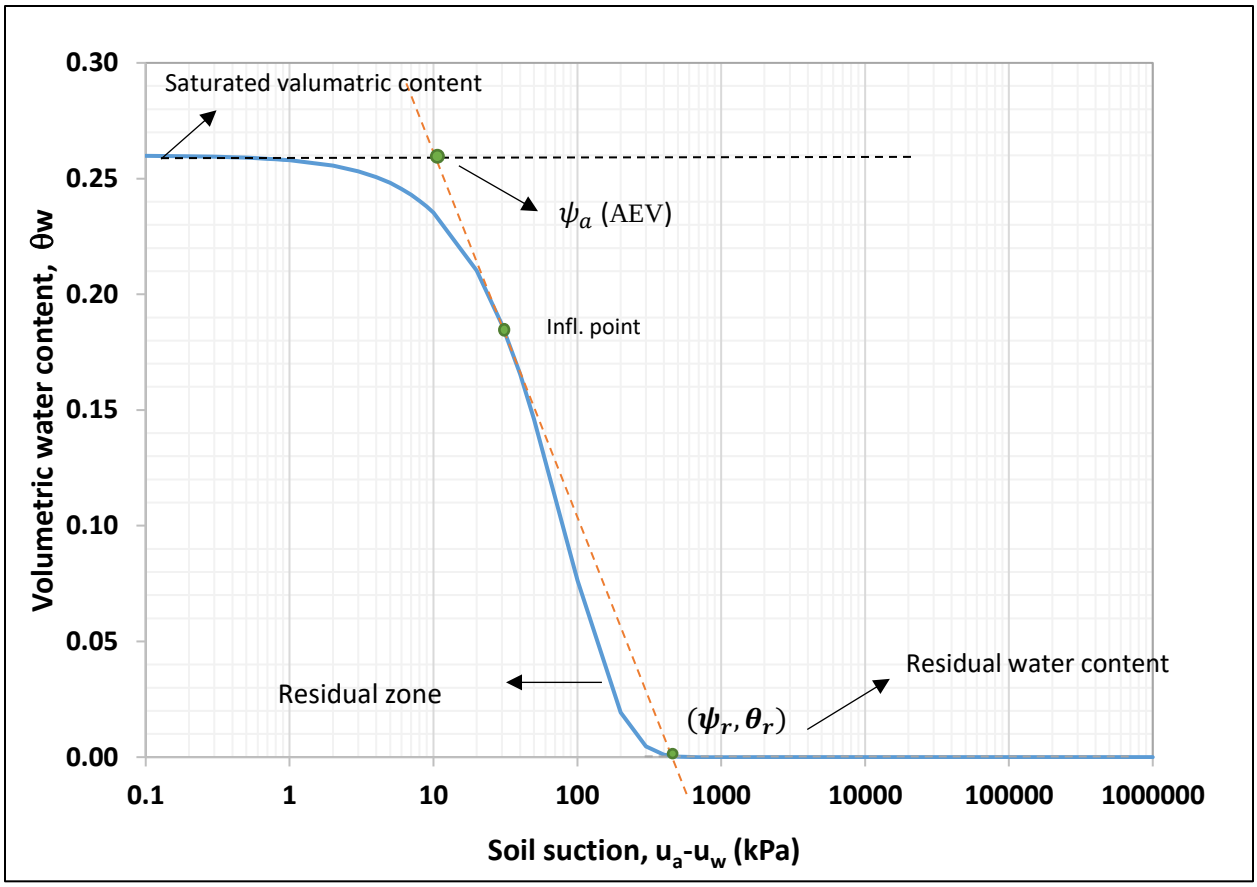

Figure 4-8 SWCC for sand soil

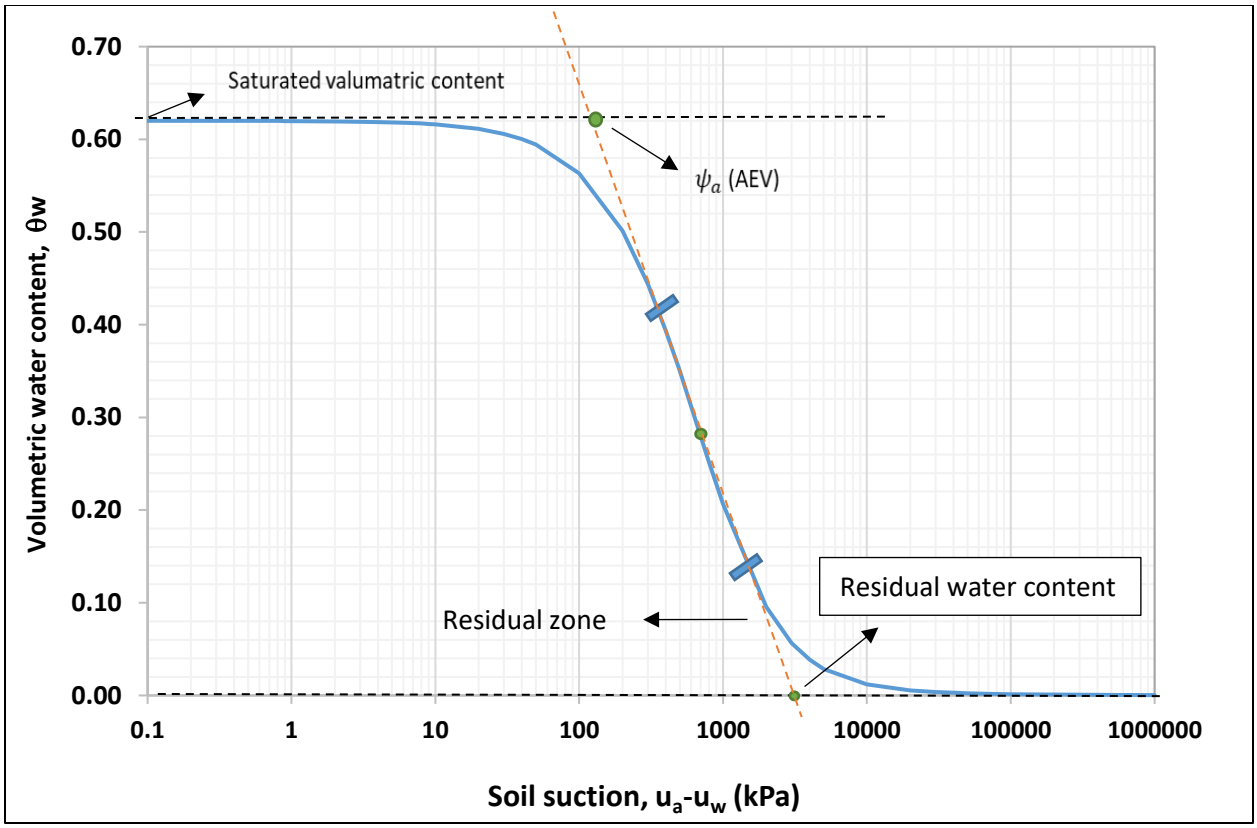

Figure 4-9 SWCC for kaolin soil

4.2.3 Shear strength properties of the soil:

By completing the three stages of the triaxial test for the course and fine-grained soil the following soil properties shown Tables 4-5 and 4-6 are obtained.

Table 4-5 Fine-grained soil kaolin shear strength data from the triaxial test.

Description	Symbol	Value	Unit
Cohesion	c’	18	kPa
Friction angle	ϕ'	23	Degree
Unit weight	γ	14	kN/m3
Phb	ϕ^b	11.5	Degree

Table 4-6 Coarse-grained soil sand shear strength data from triaxial test

Description	Symbol	Value	Unit
Cohesion	c’	0	kPa
Friction angle	ϕ'	45	Degree
Unit weight	γ	15	kN/m3
Phb	ϕ^b	22.5	Degree

4.3 Result from analytical calculation

The changes in saturation degree with depth are seen in Figure 4-10. The groundwater table was assumed to be 10 m below the surface when this map was created. According to Figure 4-11, it was thought that the soil suction or negative pore-water pressure was hydrostatic. It is clear that the ground surface had a maximum suction of 100 kPa. Ten (10) layers of dirt, each 1 meter thick, were placed between the ground surface and the groundwater table. In order to compute shaft capacity using the principles of unsaturated soil mechanics, the fluctuations of the degree of saturation and soil suction that were estimated based on SWCC results from hyprop tests for sand and kaolin were integrated in Equation 2. Equation 1 was used to get the shaft capacity using the traditional technique.

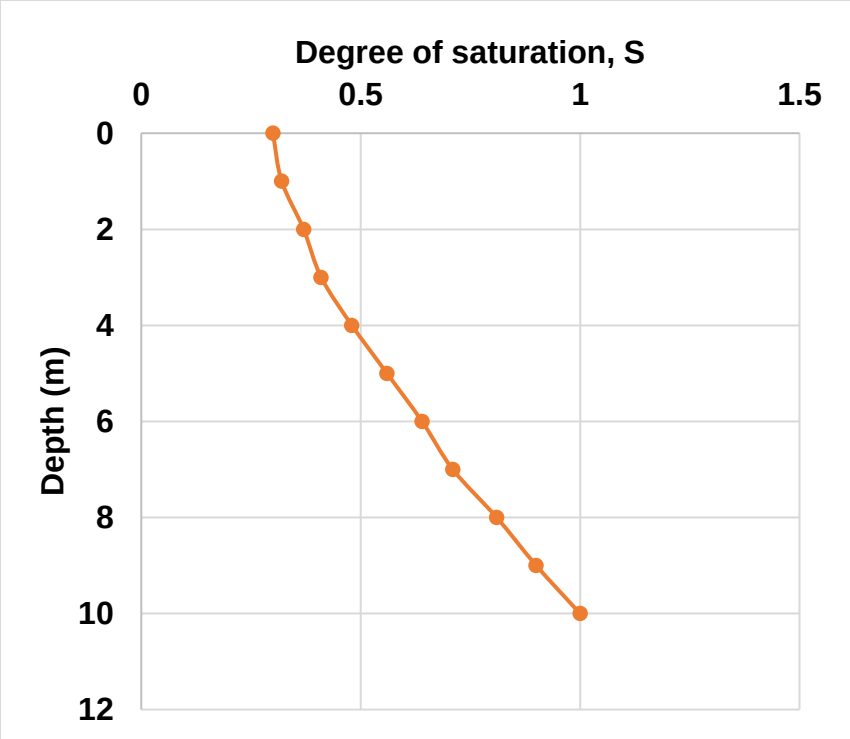

Figure 4-10 Variations of the degree of saturation with depth

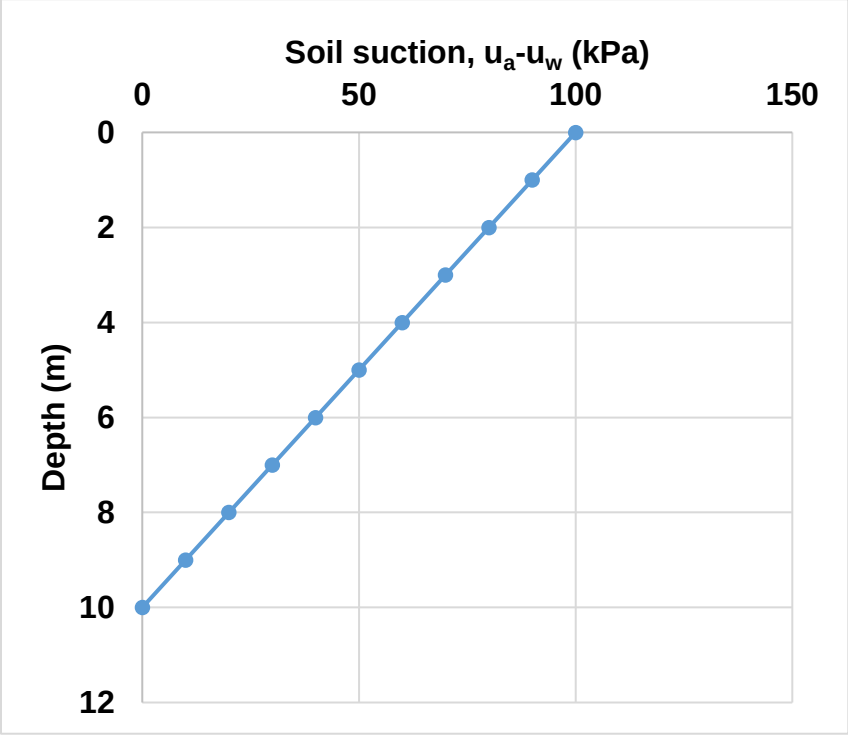

Figure 4-11 Variations of soil suction with depth

The analytical calculations show that the effective stress and matric suction significantly boost the pile foundation's shaft capacity. Based on the fluctuation of shear strength and vertical effective stress concerning matric suction, which can be calculated from SWCC and effective shear strength parameters, the updated technique is utilized to calculate the shaft capacity. (Vanapalli, Taylan 2012). Figures 4-12 and 4-22, respectively, show comparisons of shaft capacity between the standard approach and the modified method for coarse- and fine-grained soil. The computation was performed using the pile's length and the groundwatere's depths of 10 meters, 8 meters, 6 meters, 4 meters, and 2 meters. It demonstrates that in both instances, the shaft capacity determined using the modified approach produced a greater result than the old way.

According to analytical calculations and a comparison of the conventional and modified methods for coarse-grained soil (sand), the maximum shaft capacity of a 10-meter pile is at a depth of 5 meters, where it is 1180 KPa in the conventional method and 1280 KPa in the modified method, showing a difference of 100 KPa in shaft capacity between these two methods as shown in figure 4-12a. Similarly, for pile foundations with an 8-meter length, the maximum shaft capacity is at the foundation's 4-meter depth, where it is 820 KPa using the modified approach and 750 KPa using the conventional way. This difference of 70 KPa between the two methods is seen in fFigure4-12b. Figure 4-12c shows a 50 KPa difference between the two ways for a foundation that is 3 meters deep and 6 meters long. The two methods' differences are 430 and 470 kPa for traditional and modified approaches, respectively. According to Figure 4-12d, the maximum shaft capacity for a pile 4 meters long and 2 meters deep using the conventional approach is 185 KPa, whereas the maximum shaft capacity using the modified method is 120 KPa. Last but not least, figure 4-12e illustrates the maximum shaft capacity of a 2-meter pile foundation at 1 m depth, which is 47 KPa and 53 KPa for standard and modified approaches, respectively.

When there is a 10m-long pile foundation, the maximum shaft capacity for sand using the modified beta approach is 1280 KPa at a depth of 5 m.

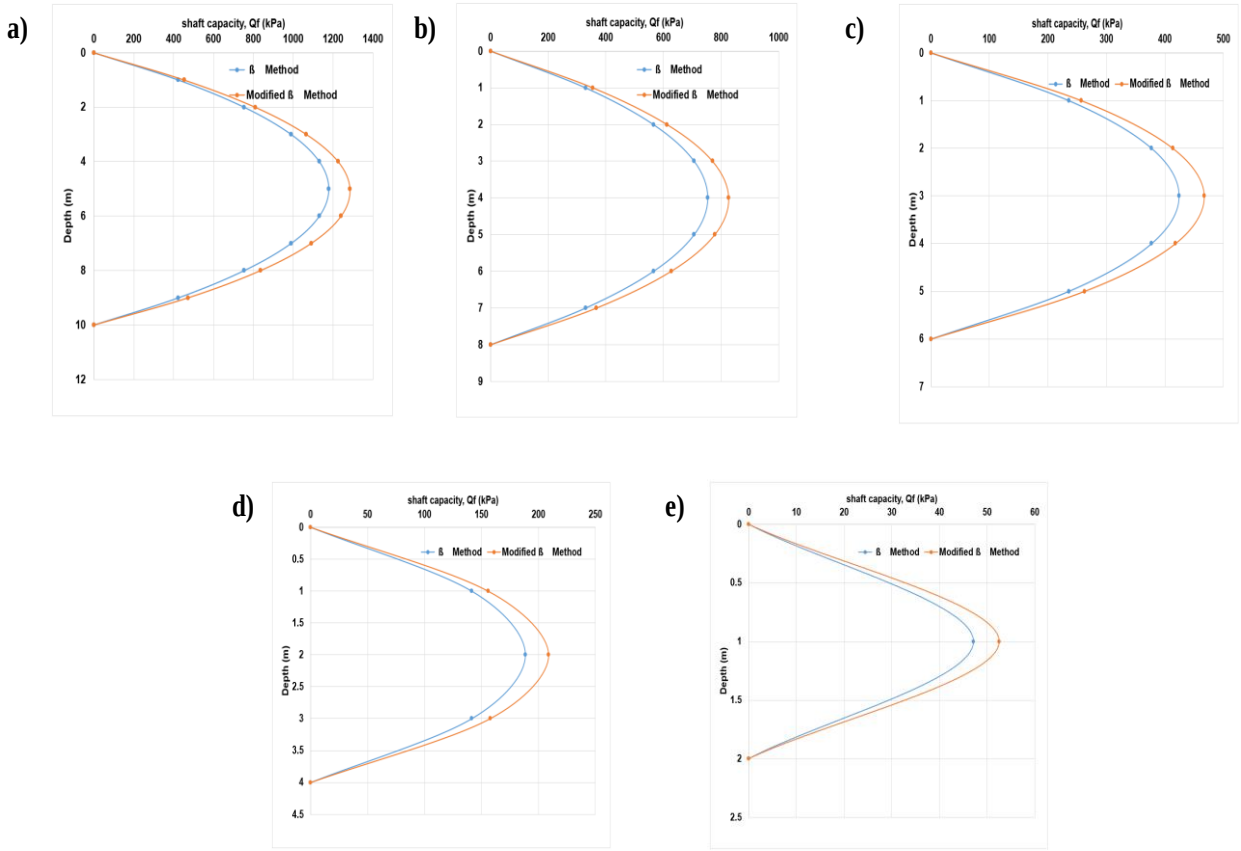

Figure 4-12 Shaft capacity, of course-grained soil based on β and modified β method

According to analytical calculations and a comparison of the conventional and modified methods for the fine-grained soil (kaolin), the maximum shaft capacity of a 10-meter pile is at a depth of 5 meters, where it is 240 KPa in the conventional method and 340 KPa in the modified method, showing a difference of 100 KPa in shaft capacity between the two methods (see figure 4-13a). Similarly, for pile foundations with an 8-meter length, the maximum shaft capacity is at the foundation's 4-meter depth, where it is 150 KPa using the traditional technique and 130 KPa using the modified method. This difference of 70 KPa between the two ways is seen in Figure 4-13b. Figure 4-13c shows a 50 KPa difference between the two ways for a foundation with a 3m depth and a 6m length of piles. The two methods' differences are 85 kPa and 130 kPa, respectively. According to Figure 4-13d, the maximum shaft capacity for a pile 4 meters long and 2 meters deep using the conventional approach is 35 KPa, whereas the maximum shaft capacity using the modified method is 60 KPa. Finally, figure 4-13e indicates a 6 KPa difference between the maximum shaft capacities for a 2-meter pile foundation at 1 m depth, which are 9 KPa and 15 KPa for traditional and modified approaches, respectively.

When there is a 10m-long pile foundation, the maximum shaft capacity of kaolin using the modified beta technique for sand is 340 KPa.

The lower size of the pile may be created to maximize the construction of the foundation using a modified technique including effective stress and matric suction, it can be inferred from calculations utilizing beta methods.

When compared to fine-grained soil, the analytical calculation utilizing the beta approach shows that coarse-grained soil creates a greater shaft capacity of the pile. Due to the reduced effective stress in the fine-grained soil, the maximum shaft capacity of a 10-meter pile is 340 kPa as opposed to 1280 KPa in coarse-grained soil.

Figures 4-12 and 4-13 illustrate how standard and modified approaches differ for both coarse and fine-grained soil. It is 100 KPa, 70 KPa, 50 KPa, 25 KPa, and 6 KPa for pile foundations with lengths of 10 m, 8 m, 6 m, 4 m, and 2 m.

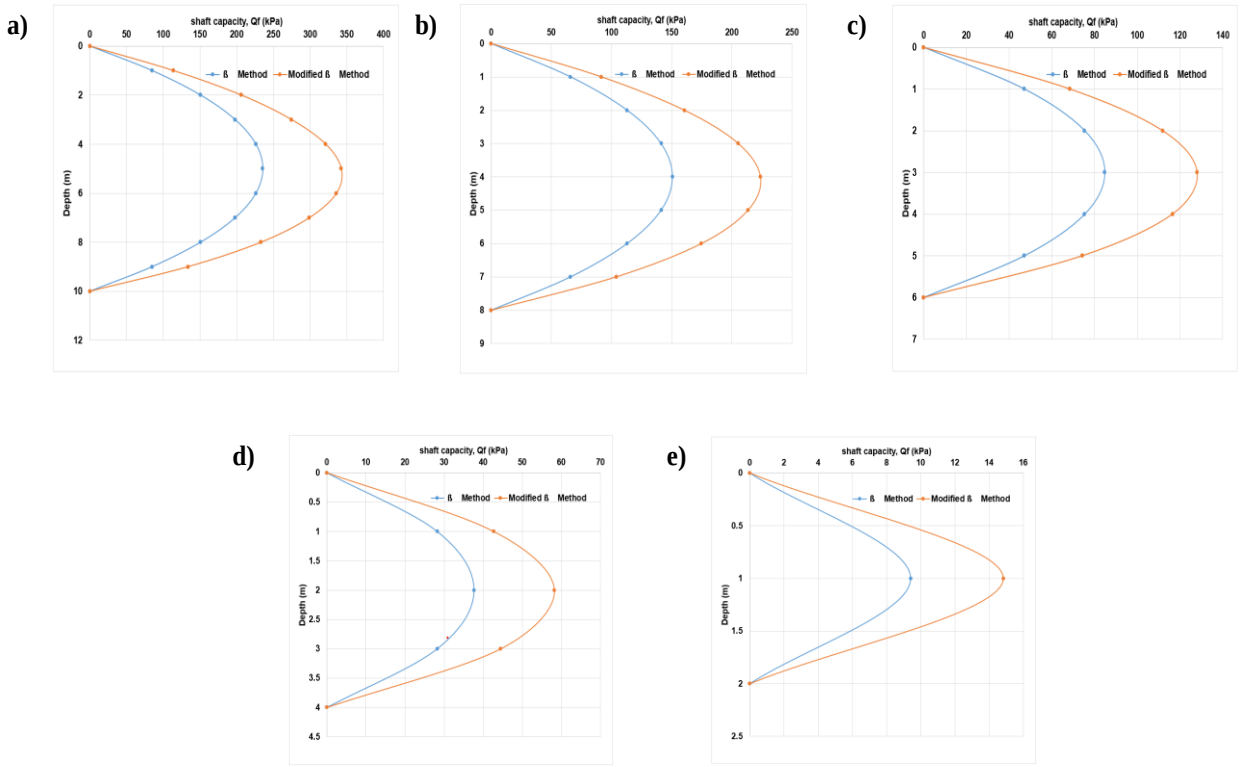

Figure 4-13 Shaft capacity of fine-grained soil based on β and modified β method

Based on SWCC and the undrained shear strength of the soil, the modified approach is utilized to calculate the fluctuation of shaft capacity concerning matric suction. (Vanapalli et. al. 2012). The calculation's outcome for calculating the shaft capacity of piles shows that the modified approach, which differs most from its conventional counterpart in calculations for both fine- and coarse-grained soils, yields the lowest value for shaft capacity when compared to modified and modified methods.

Figures 4-14 and 4-15 show comparisons of shaft capacity between the standard approach and the modified method for coarse- and fine-grained soil, respectively. The depths of the groundwater table at 10, 8, 6, 4, and 2 meters, as well

as the lengths of the pile at 10, 8, 6, 4, and 2 meters, were used in the analytical calculations. It demonstrates that the updated approach produced a greater number for the shaft capacity calculation than the original method.

Both fine-grained and coarse-grained soils have the same soil qualities that are taken into account by the alpha technique. As can be seen in Figures 4-14 and 4-15, the findings for both types of soil are therefore identical.

The maximum shaft capacity of a 10-meter pile is at a depth of 7 meters, where it is 60 KPa in the conventional method and 135 KPa in the modified method, showing a difference of 165 KPa in shaft capacity between these two methods, as shown in figures 4-14a and 4-15a. This calculation was done analytically and compared the conventional and modified alpha methods for the coarse-grained soil (sand) and fine-grained soil (kaolin). Similarly, for a pile foundation with an 8-meter length, the maximum shaft capacity is at the foundation's 6-meter depth, where it is 58 KPa using the traditional technique and 158 KPa using the modified method. This difference of 100 KPa between the two ways is seen in Figures 4-14b and 4-15b. Figures 4-14c and 4-15c indicate a 100 KPa difference between the two approaches for a foundation with a 6 m long pile, which differ by 35 kPa and 135 kPa for traditional and modified methods, respectively. The maximum shaft capacity for a pile 4 meters long and 3 meters deep using the standard approach is 25 KPa, whereas the maximum shaft capacity using the modified method is 55 KPa, a difference of 30 KPa. Finally, figure 4-14e and Figure 4-15e illustrate the maximum shaft capacity of a 2-meter pile foundation at 1.5 m depth, which is 14 KPa and 20 KPa for traditional and modified approaches, respectively.

When there is a 10m-long pile foundation, the maximum shaft capacity for sand and kaolin using the modified alpha technique is 135 KPa.

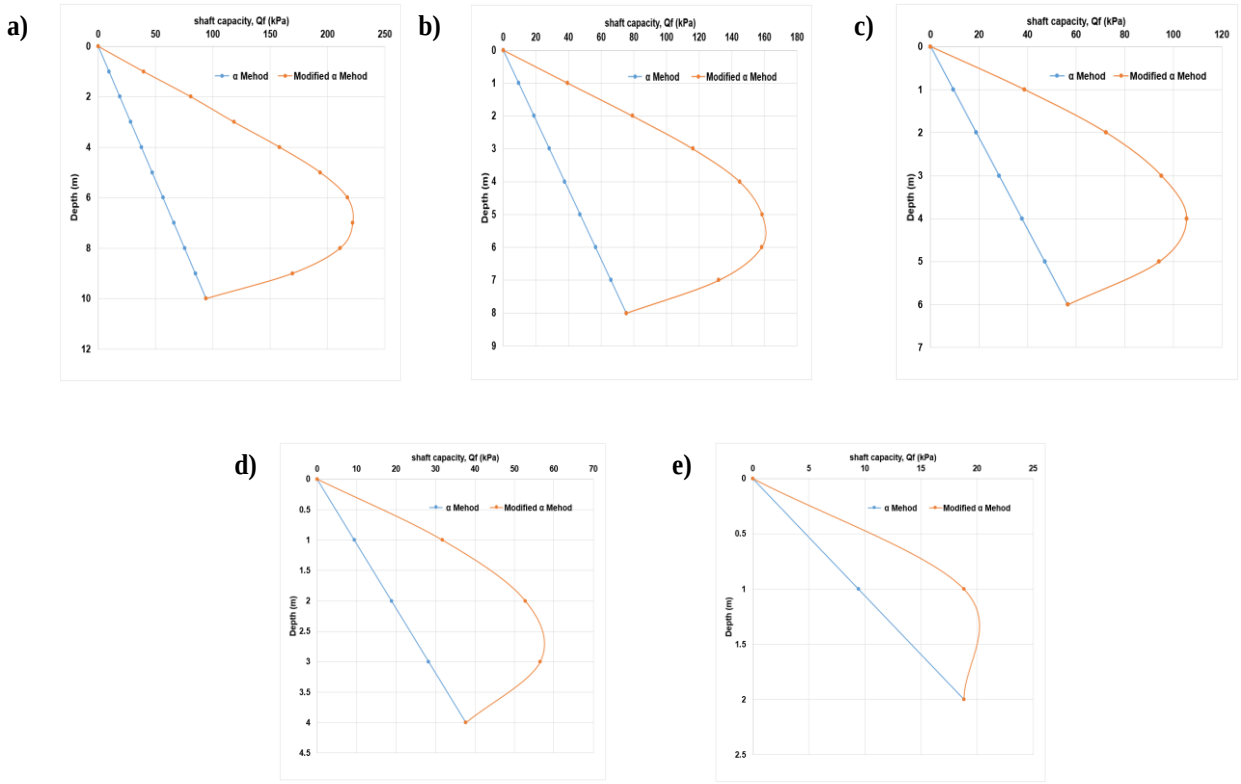

Figure 4-14 Shaft capacity coarse-grained soil based on α and modified α method

According to the calculations using alpha methods, it can be deduced that the smaller size of the pile can be designed to optimize the design of the foundation using a modified method incorporating the matric suction.

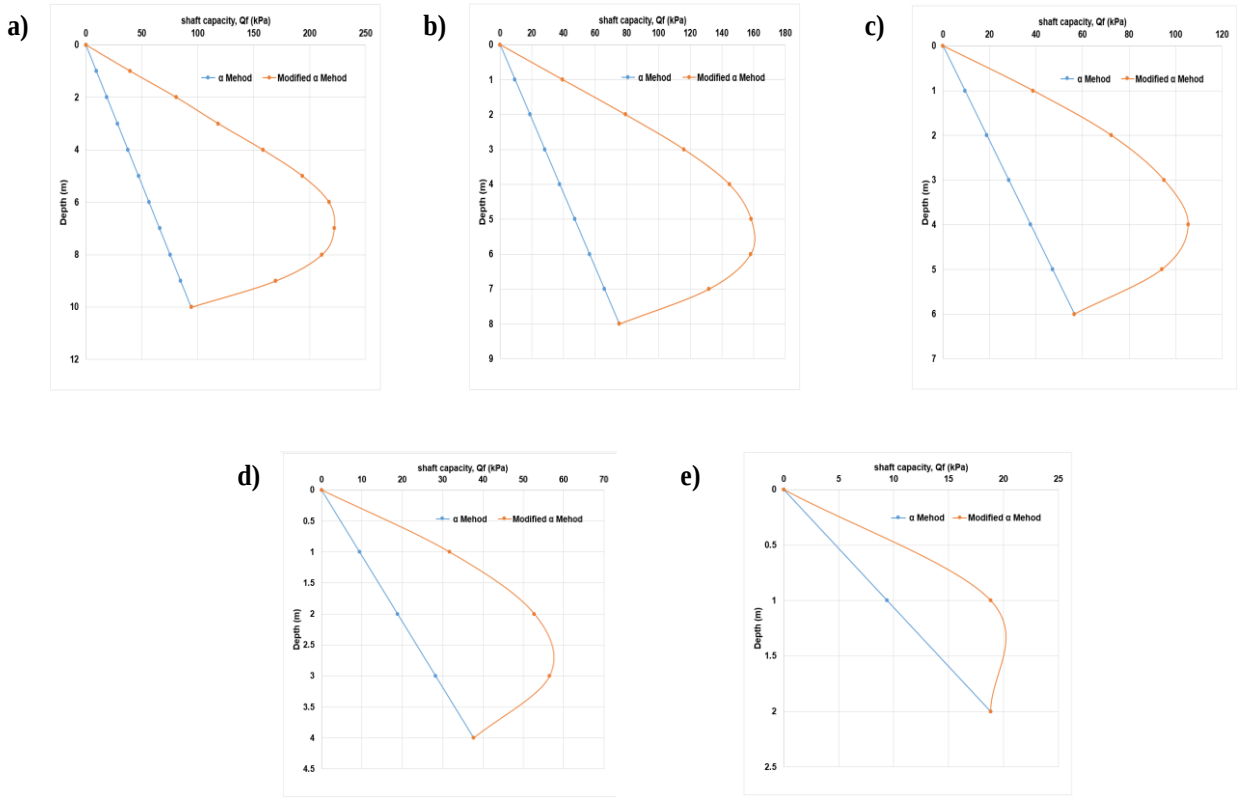

Figure 4-15 Shaft capacity fine-grained soil based on α and modified alpha method

Figure 4-16 compares the shaft capacity of coarse-grained soil between the original approach and the improved method, whereas Figure 4-17 compares the shaft capacity of fine-grained soil. The depths of the groundwater table at 10, 8, 6, 4, and 2 meters, as well as the lengths of the pile at 10, 8, 6, 4, and 2 meters, were used in the analytical calculations. It demonstrates that the updated approach produced a greater number for the calculated shaft capacity compared to the original method.

The traditional method's maximum shaft capacity for a 10-meter pile is 320 KPa, while the modified lambda method's maximum capacity is 570 KPa for coarse-grained soil at a depth of 6 meters. (sand). Figure 4-16a illustrates this difference in shaft capacity between the two approaches, which is 160 KPa. Similar to this, the maximum shaft capacity for an 8-m-long pile foundation is at the foundation's 5-m depth, where it is 130 KPa with the traditional methodology and 360 KPa with the updated method. Figure 4-16b illustrates the 140 KPa pressure differential between the two methods. For a foundation with a 6 m long pile, Figure 4-16c illustrates a 50 KPa difference between the two ways, compared to 140 KPa and 200 KPa for the traditional and modified procedures, respectively. Figure 4-16d

shows that the conventional method's maximum shaft capacity for a pile of 4 meters in length and 3 meters in depth is 75 kPa, whereas the modified method's maximum shaft capacity is 95 kPa. According to Figure 4-16e, the maximum shaft capacity of a 2 m pile foundation is, at 1 m depth, 16 KPa for traditional techniques and 30 KPa for modified methods, respectively. When there is a 10m-long pile foundation, the maximum shaft capacity for sand using the modified beta approach is 570 KPa at a depth of 6m.

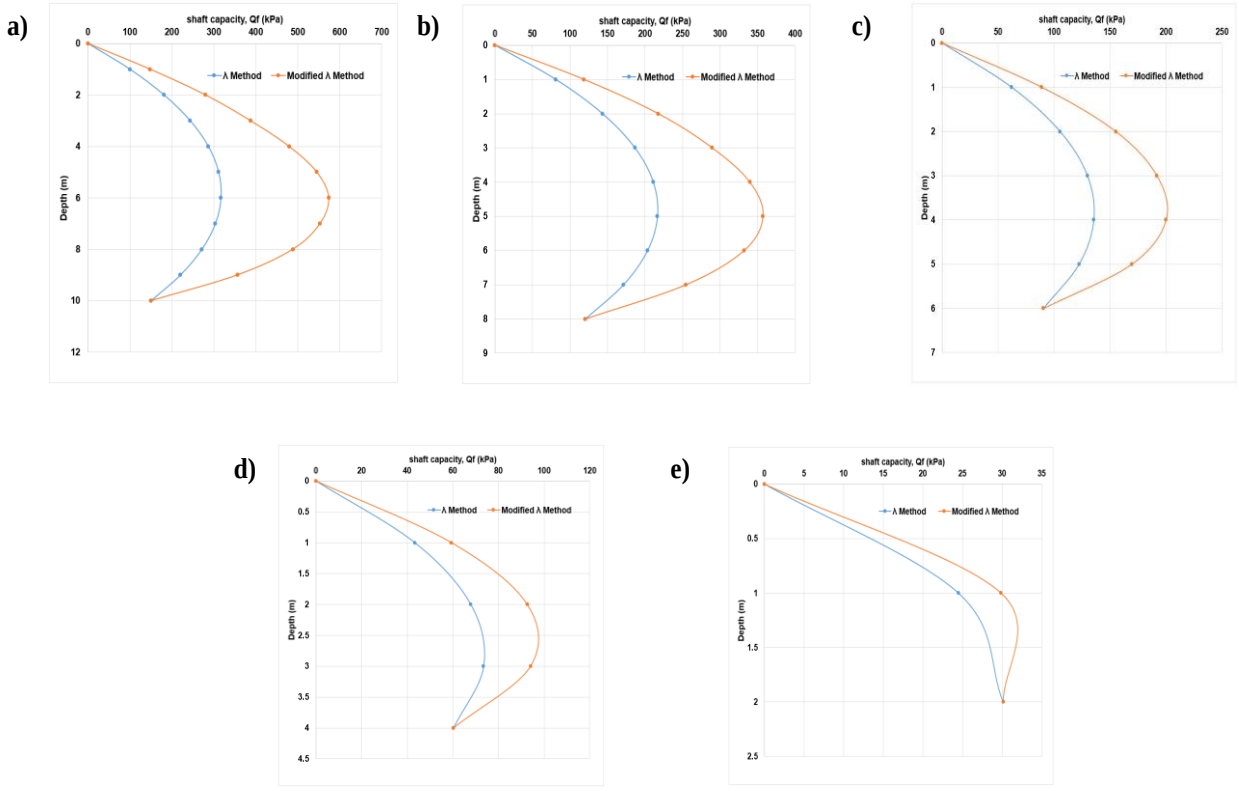

Figure 4-16 Shaft capacity of coarse-grained soil based on λ and modified lambda method

The maximum shaft capacity of a 10-meter pile is at a depth of 6 meters, where it is 190 KPa in the conventional method and 440 KPa in the modified method, showing a difference of 160 KPa in shaft capacity between these two methods. This is according to analytical calculations and a comparison of the conventional and modified methods for the fine-grained soil (kaolin). (see Figure 4-17a). Similar to this, for an 8-meter-long pile foundation, the maximum shaft capacity is 130 KPa using the conventional methodology and 270 KPa using the modified method at the foundation's 5-meter depth. Figure 4-17b illustrates the 140 KPa difference between the two approaches. The two procedures for a foundation with a 6 m long pile are shown to differ by 90 kPa and 150 kPa in Figure 4-17c for traditional and modified methods, respectively. The standard method's maximum shaft capacity for a pile that is 4 meters long and 3 meters deep is 58 kPa, whereas the updated method's maximum shaft capacity is 78 kPa. Figure 4-17d illustrates the 20 kPa difference between the two methods. The maximum shaft capacity of a 2 m pile foundation

at 1 m depth is shown in Figure 4-17e, which is 19 KPa for traditional methods and 15 KPa for modified approaches, respectively.

The maximum shaft capacity of kaolin utilizing the modified lambda technique for sand is 440 KPa when there is a 10 m-long pile foundation.

It may be deduced from calculations using beta approaches that the lower side of the pile can be made to maximize the building of the foundation using a modified method that includes effective stress and matric suction.

Coarse-grained soil creates a pile with a greater shaft capacity than fine-grained soil, according to an analytical calculation utilizing the lambda approach. The maximum shaft capacity of a 10-meter pile is 440 kPa as opposed to 570 kPa for coarse-grained soil because of the decreased effective stress in fine-grained soil.

The differences between conventional and modified procedures for both coarse- and fine-grained soil are shown in Figures 4-16 and 4-17. It varies from 160 KPa to 140 KPa to 60 KPa to 20 KPa to 5 KPa, depending on how long the pile foundation is.

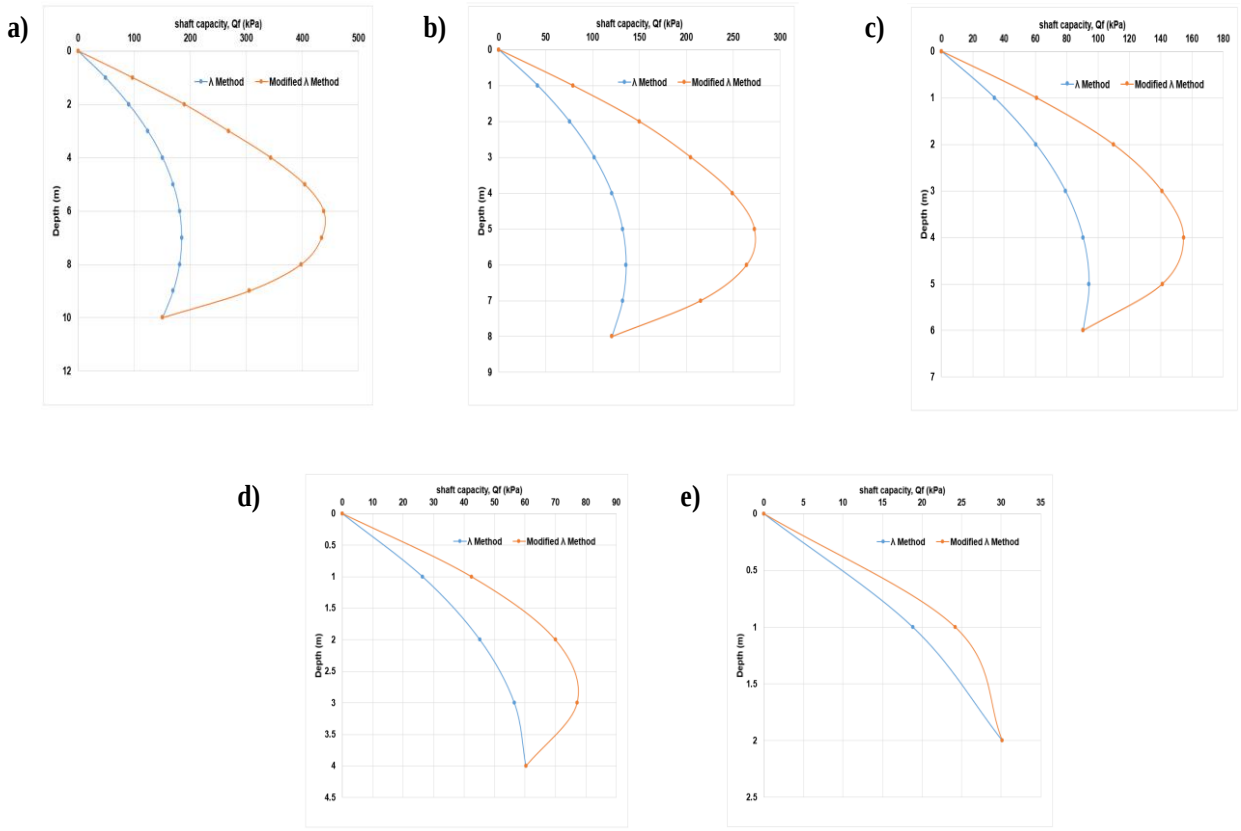

Figure 4-17 Shaft capacity of fine-grained soil based on λ and modified lambda method

4.4 Result of Numerical analyses using plaxis 3D:

Figure 4-18 illustrates the 3D modeling of the pile using Plaxis 3d. the length of the pile is assumed 10 m and the depth of the groundwater table is 10m too.

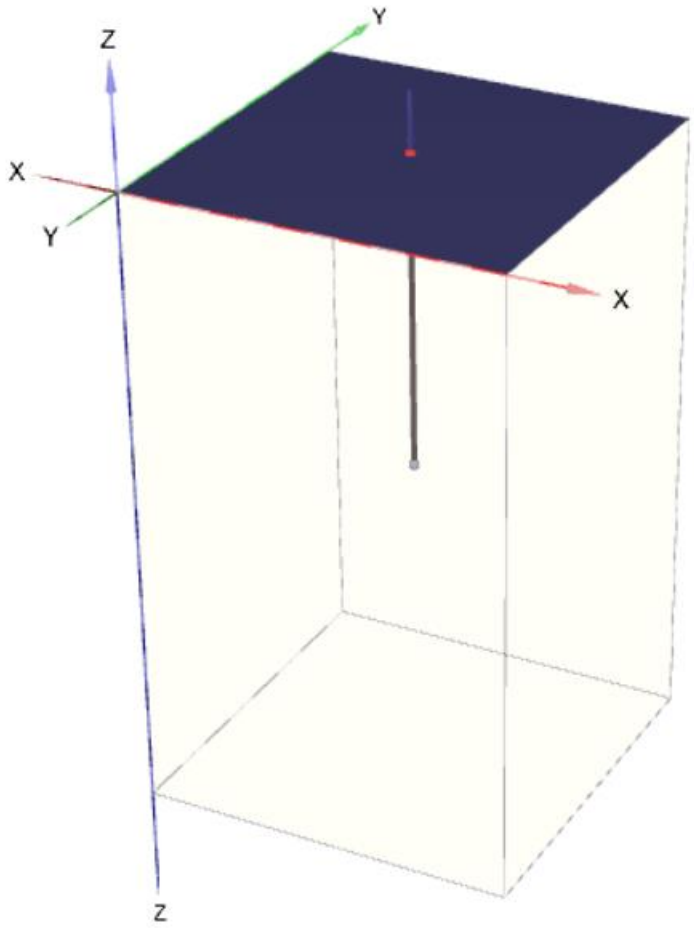

Figure 4-18. 3D model of pile foundation in sand using Plaxis

4.4.1 Result of numerical analyses for coarse-grained soil (Sand):

For numerical analyses in this research work, Plaxis 3D is used. The data for this calculation was obtained from laboratory testing mentioned in this research paper and also from some related research papers.

Table 4-7 Laboratory data used for foundation modeled in sandy and Kaolin soil using plaxis 3D

Soil type	Sand
Soil Model	Mohr-Coulomb
Drainage Type	Drained
Unsaturated unit weight	16 KN/ m^3
Saturated unit weight	20 KN/ m^3
Void ratio	0.71
Modules of elasticity	430 KN/ m^3
Cohesion	0
Friction angle	45

Rainfall-related variation in suction was examined. For the sake of this computation, a 10m pile length is used. 12 days of rain are followed by 12 days without rain. 20 millimeters of rainfall each day in Astana, Kazakhstan. The largest amount of precipitation is 12 days at 20mm per day. (Zhussupbekov et al., 2018). The amount of rainfall and the time interval of rainfall may be entered in the attribute library during the stage creation phase of modeling using Plaxis. Editing the flow function in the arbitrary library will let you add the discharge function, which will allow you to add the time and quantity of precipitation (see Figure 4-19). According to the outcome of the numerical calculations, rainfall penetration in both fine- and coarse-grained soil causes a decrease in suction. For coarse-grained soil (Sand), the initial suction is 100 kPa (before rainfall infiltration), declining to 80 kPa after one day of continuous rain, 30 KPa after 12 days, and 10 KPa after the time. This shows that even after 12 days of rain, water continues to flow into the water table, lowering the negative pore water pressure. Additionally, due to rainfall, the groundwater table depth decreases from its original assumption of 10 meters to 9 meters after the time. The outcome also shows that soil would weaken as a result of reduced suction.

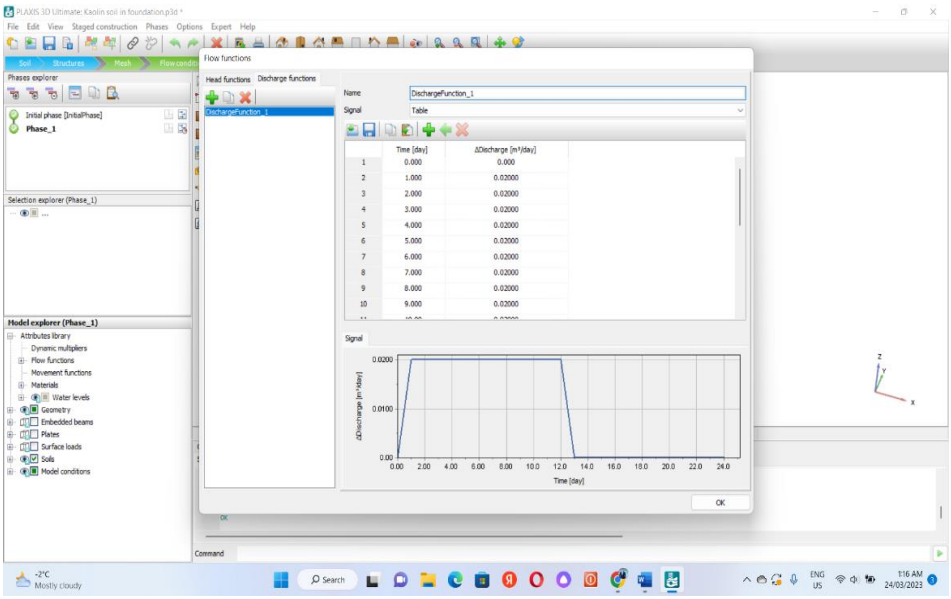

Figure 4-19 Foundation modeling using Plaxis 3D

Figure 4-20 displays a 3D representation of the foundation as well as a cross-section of a pile that was designed using Plaxis 3D. The pile's cross-section shows that moisture in the sand causes the matric suction to diminish. Before the rain, it is 100 KPa, and towards the conclusion of the period under consideration, it is 10 KPa. Additionally, it demonstrates how, as a result of water infiltration at the groundwater table and into the depths, the negative pore water pressure decreases during the 12 days of the dry time that follow the 12 days of rainfall.

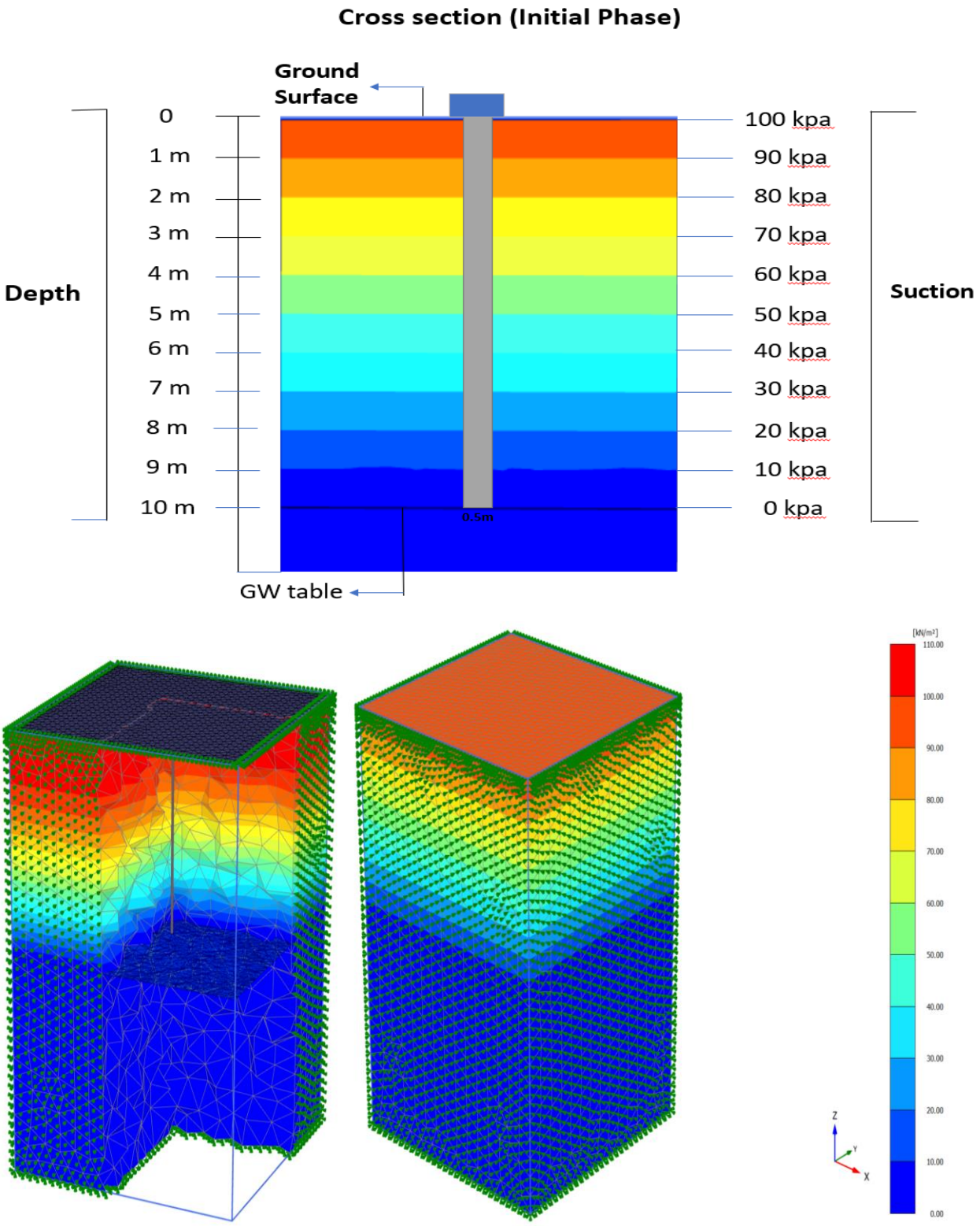

Figure 4-20 Initial phase in plaxis 3D analyses

Figure 4-21 shows how the suction at the ground's surface changes to 30 KPa after 12 days of rainfall and how it decreases to 0 KPa at groundwater table depths of 9 and 10. The shaft capacity of the pile is reduced as a result of this drop in suction.

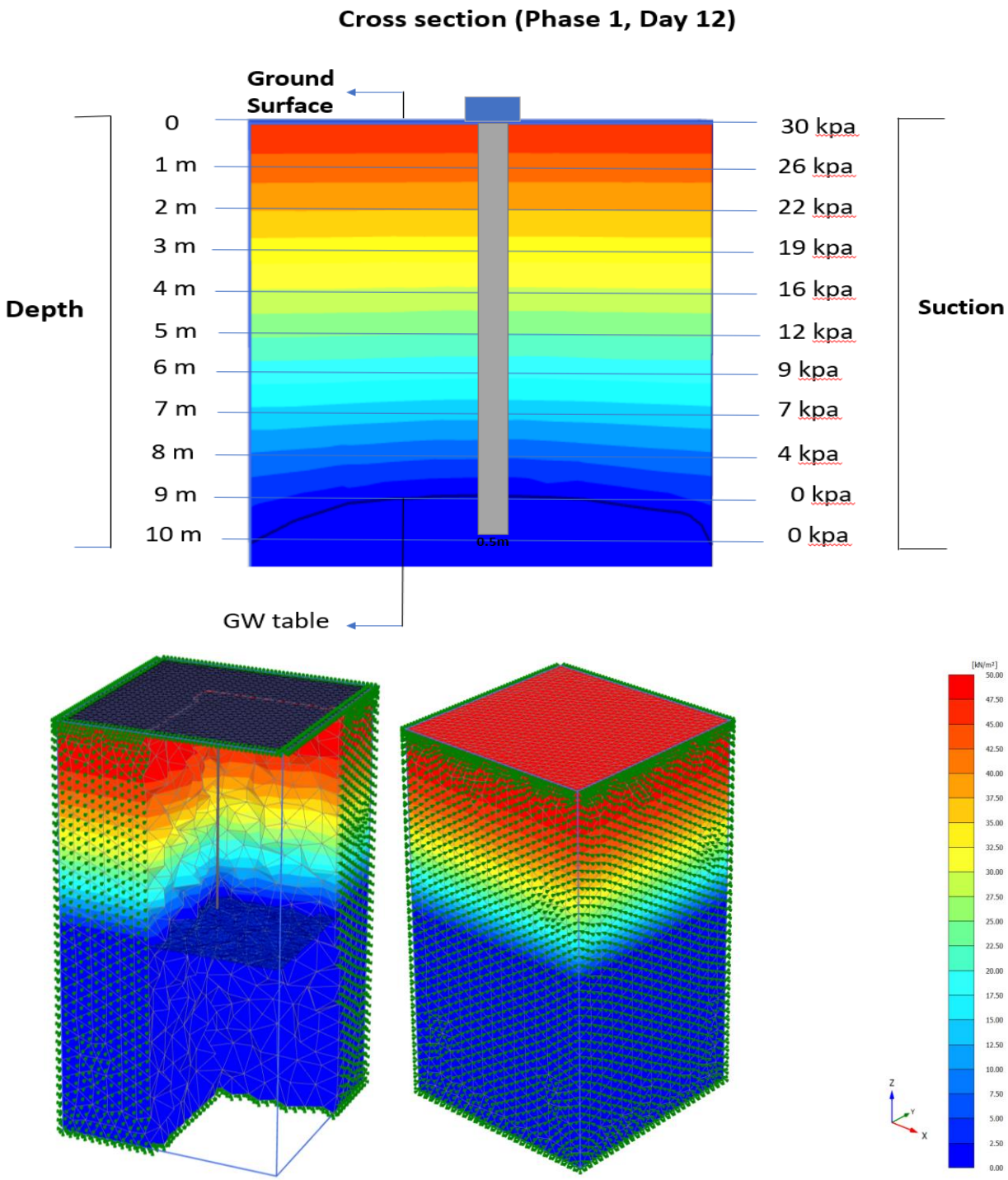

Figure 4-21 Suction variation of sand due to rainfall in plaxis 3D analyses

In the coarse-grained soil (sand), the negative pore water pressure (matric suction) diminishes during periods of rainfall and the ensuing dryness, as seen in Figure 4-22. In the first phase, the suction is operating at its maximum rate of 100 KPa. (day 0). It descends in a downward direction until it hits 10 KPa after the time. The suction fluctuation caused by rainfall in the coarse-grained soil over the course of 12 days is shown in Figure 4-23. According to the graph, there is a 30 kPa maximum suction after 12 days of rain. The suction changes throughout the 12 days following a downpour are shown in Figure 4-24. According to the graph, the maximum suction after the dry time of 12 days is 10 kPa. After 12 days of rainfall, the soil suction drops from 100 kPa to 30 kPa, and then it drops to 10 kPa after the time, showing a 70 kPa reduction in 12 days of rainfall and a 90 kPa reduction over the course of the whole 24-day period.

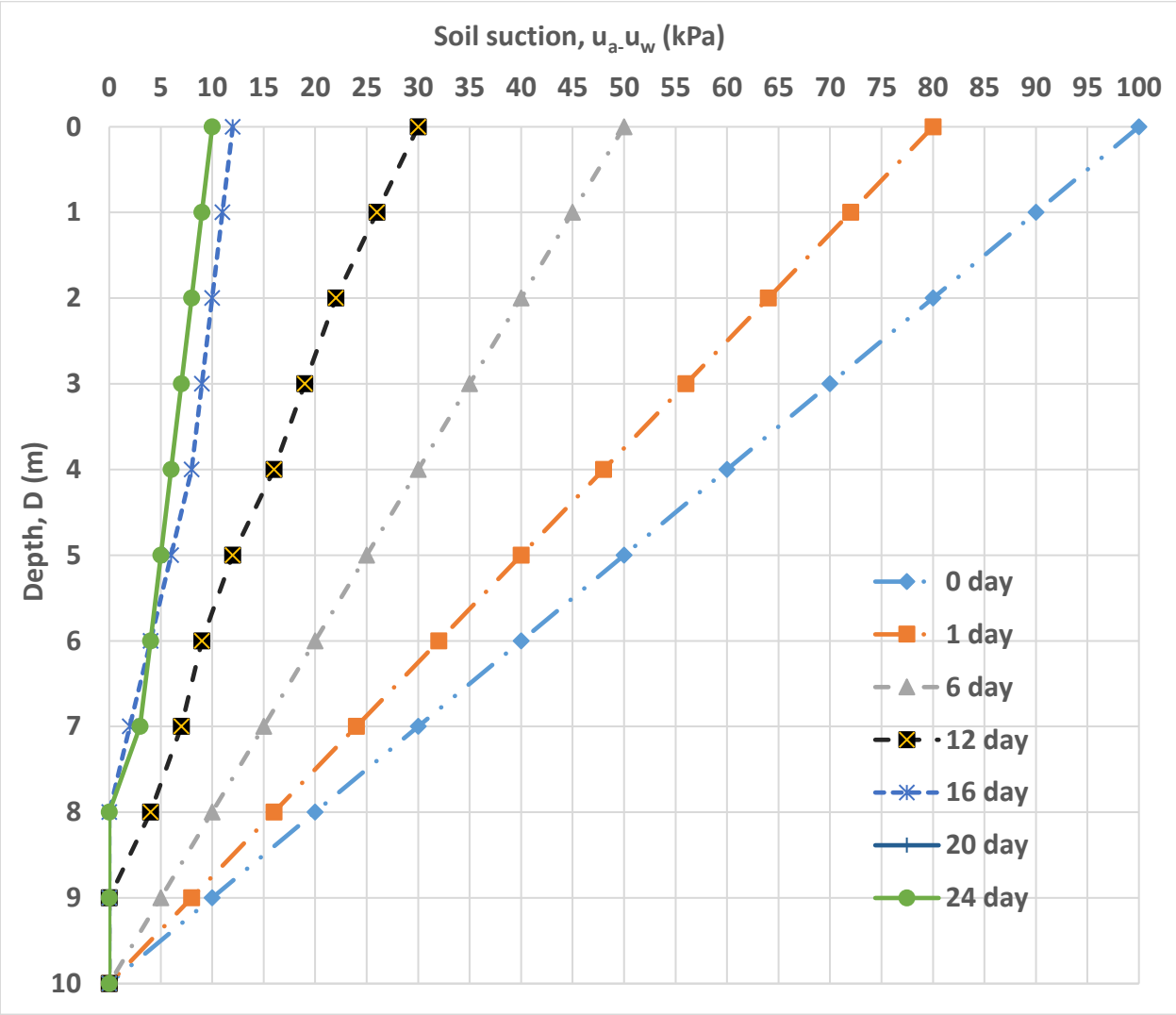

Figure 4-22 Graph of suction variation of sand due to 15 days rainfall by plaxis 3D analyses

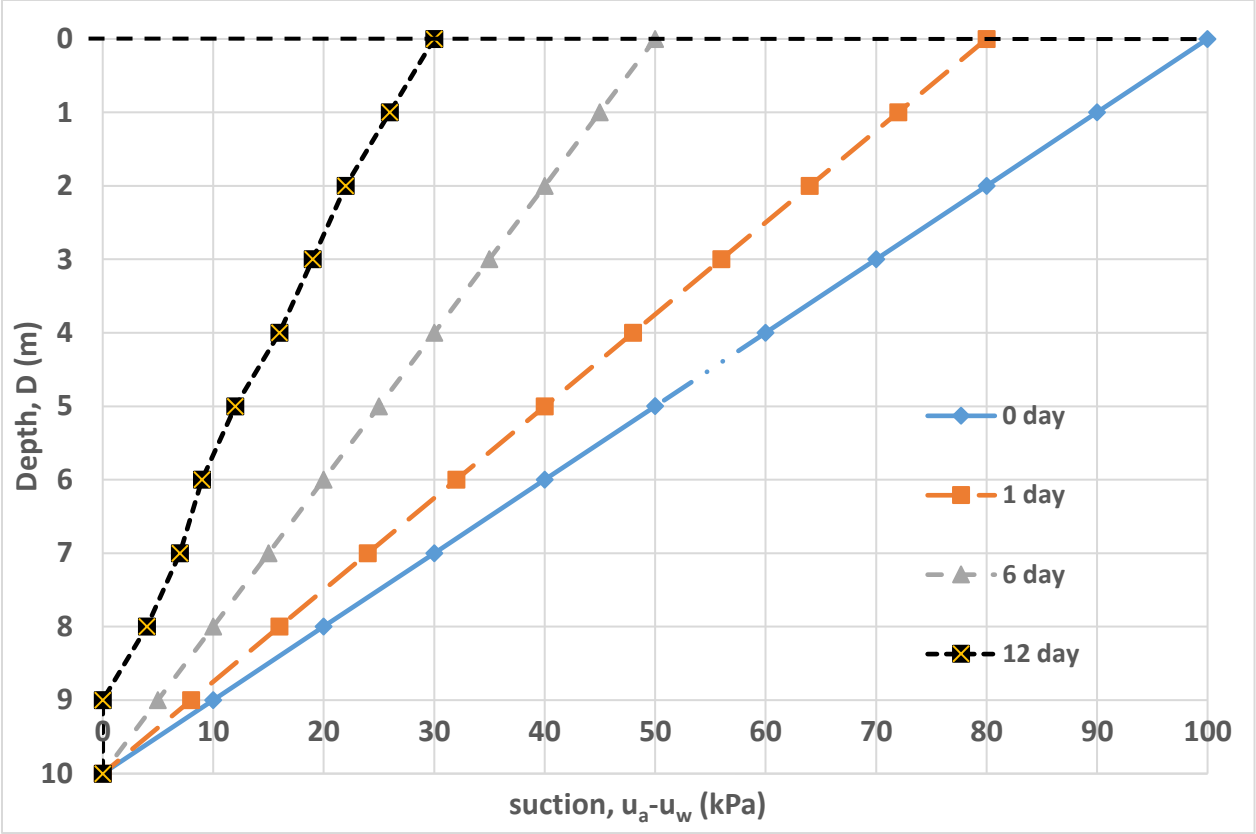

Figure 4-23 Graph of suction variation of sand due to 12 days rainfall by plaxis 3D analyses

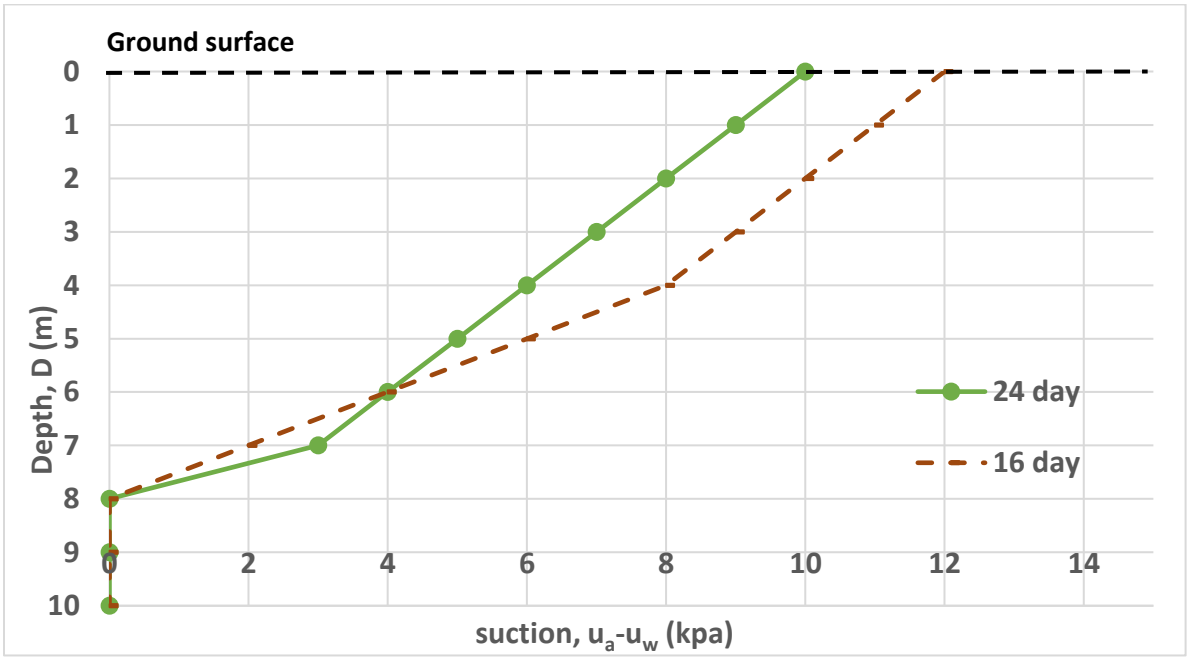

Figure 4-24 Graph of suction variation of sand due to 12 days dry period by plaxis 3D

4.4.1.1 Shaft capacity of the pile after rainfall infiltration from plaxis results for coarse grain soil (Sand):

4.4.1.1.1 Modified Beta Method:

The soil's shaft capacity will alter as a result of rainfall and variations in soil suction. The three widely used methods for calculating the shaft capacity of pile foundations were updated to include the newly discovered suction following rainfall. (Modified alpha, beta, and lambda methods). Figure 4-25 displays the results of an analytical computation using the modified Beta approach. For a foundation depth of 10m and pile length of 10m, calculations were done for the first phase (before rainfall), Day 1, Day 6, Day 12, Day 16, and Day 24. According to the results of the modified beta approach, the shaft capacity of pile foundations decreases by 90 KPa as a result of the infiltration of rainwater, going from 1320 KPa during the first phase to 1120 KPa after 12 days of rainfall. The shaft capacity falls from 1120 KPa to 1090 KPa over 12 days of dry weather, a shift of 20 KPa. This pattern indicates that, due to variations in suction, the shaft capacity decline will persist in dry periods after rainfall, but the change will be noticeably slower.

Using the modified beta approach, the analytical calculation result of sand shaft capacity after rainfall is shown in Figure 4-25.

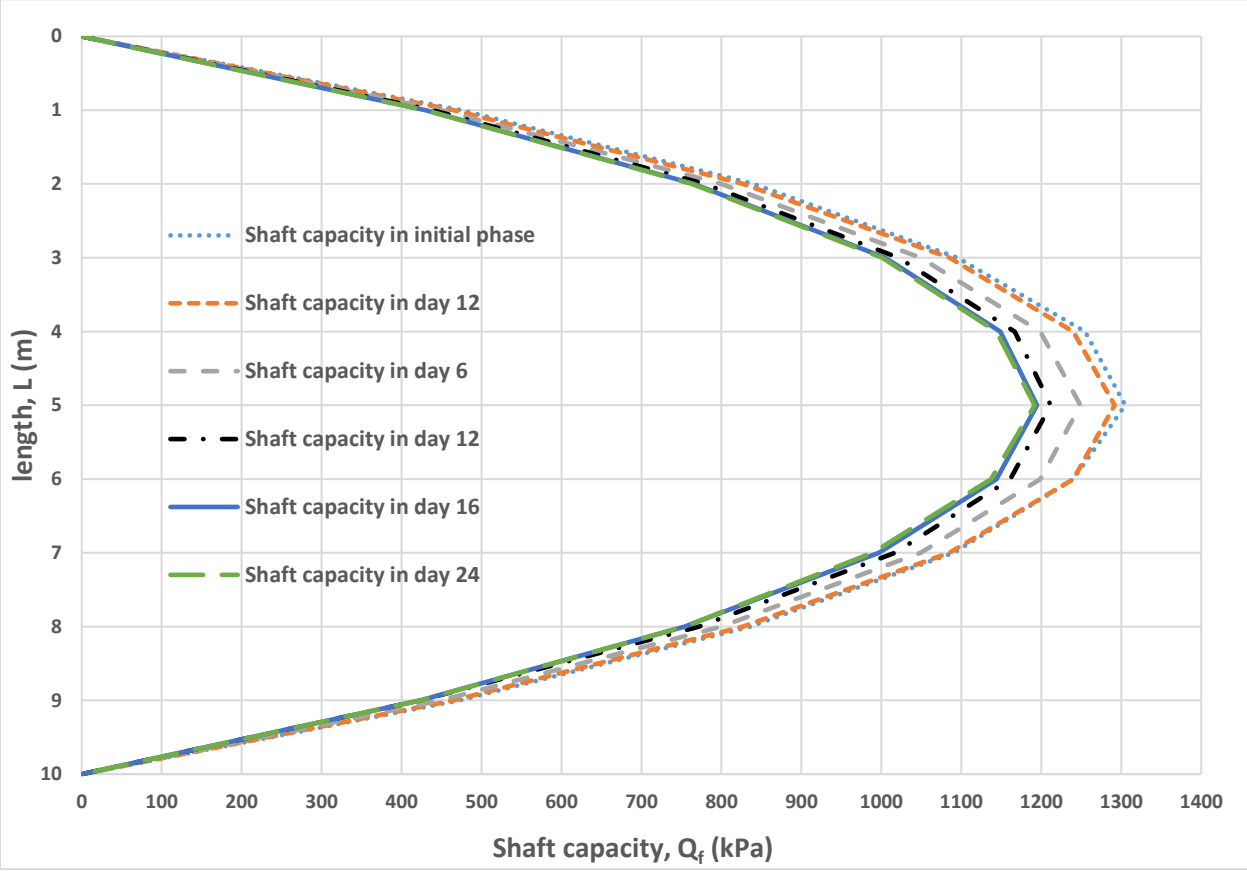

Figure 4-25 Analytical calculation of sand shaft capacity after rainfall using the modified beta

4.4.1.1.2 Modified Alpha Method:

Figure 4-26 displays the outcome of an analytical computation utilizing the modified Alpha approach. The calculations were done in 10 m of groundwater table depth and 10 m of pile length for the first phase (before rainfall), Day 1, Day 6, Day 12, Day 16, and Day 15. The modified alpha method's findings show that rainwater infiltration causes the shaft capacity of pile foundations to drop by 115 KPa, from 168 KPa in the first phase to 44 KPa after the 12-day rainy period. The shaft capacity changes from 44 KPa to 20 KPa throughout the dry period of 12 days. As a result, the shaft capacity diminishes in dry periods at a far slower rate than it does in wet periods.

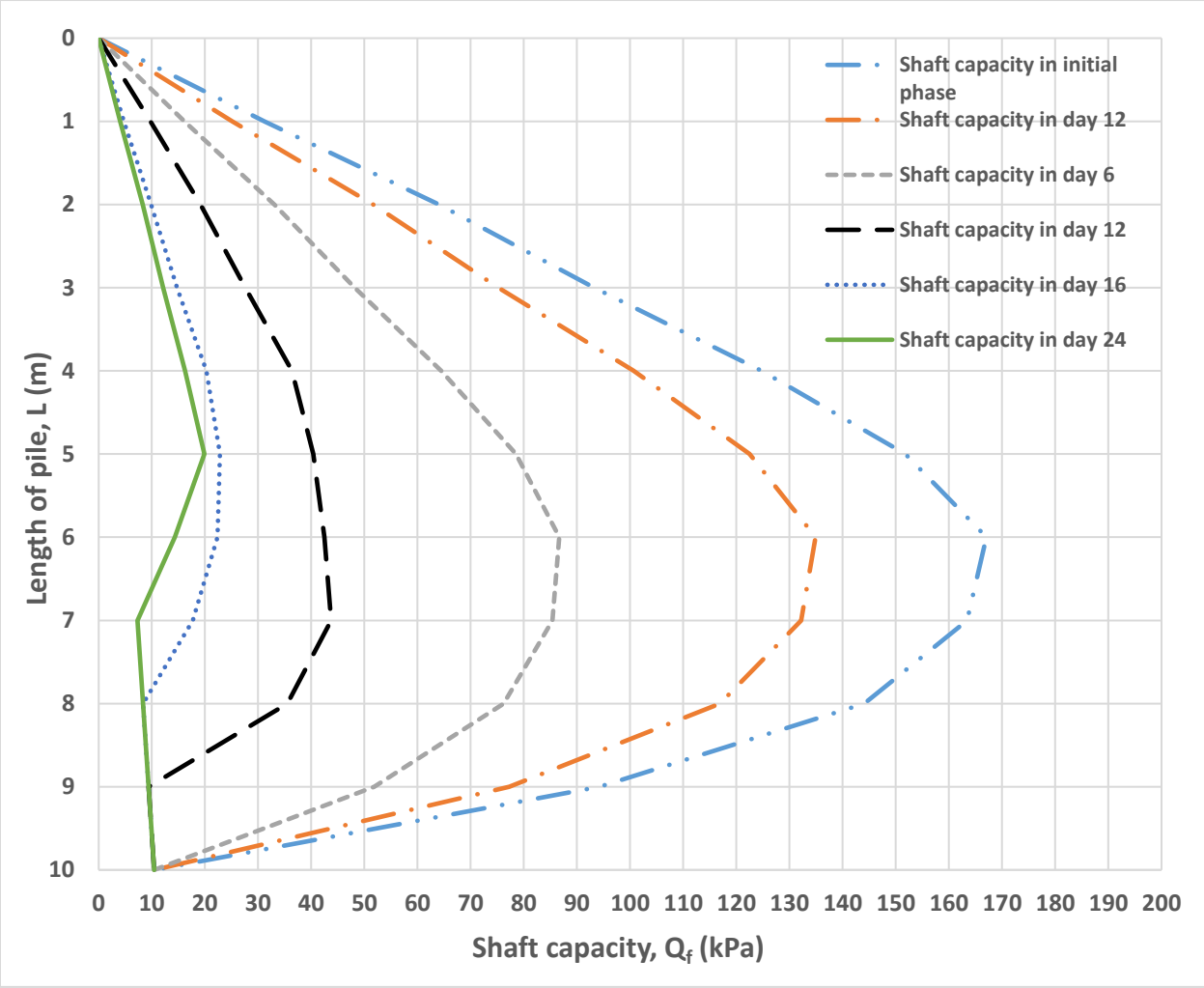

Figure 4-26. Analytical calculation result of sand shaft capacity after rainfall using the modified alpha method

4.4.1.1.3 Modified Lambda Method:

The results of an analytical computation utilizing the modified lambda approach are shown in Figure 4-27. The calculations were done in 10 m of groundwater table depth and 10 m of pile length for the first phase (before rainfall), Day 1, Day 6, Day 12, Day 16, and Day 24. According to the modified beta technique results, rainwater infiltration causes the shaft capacity of pile foundations to decrease by 650 KPa, going from 1000 KPa in the first phase to almost 350 KPa after the 12-day period. After 12 days of dry time, the shaft capacity decreased from 220 KPa at the beginning of the dry period to 130 KPa, indicating a 130 KPa variance in the pile's shaft capacity.

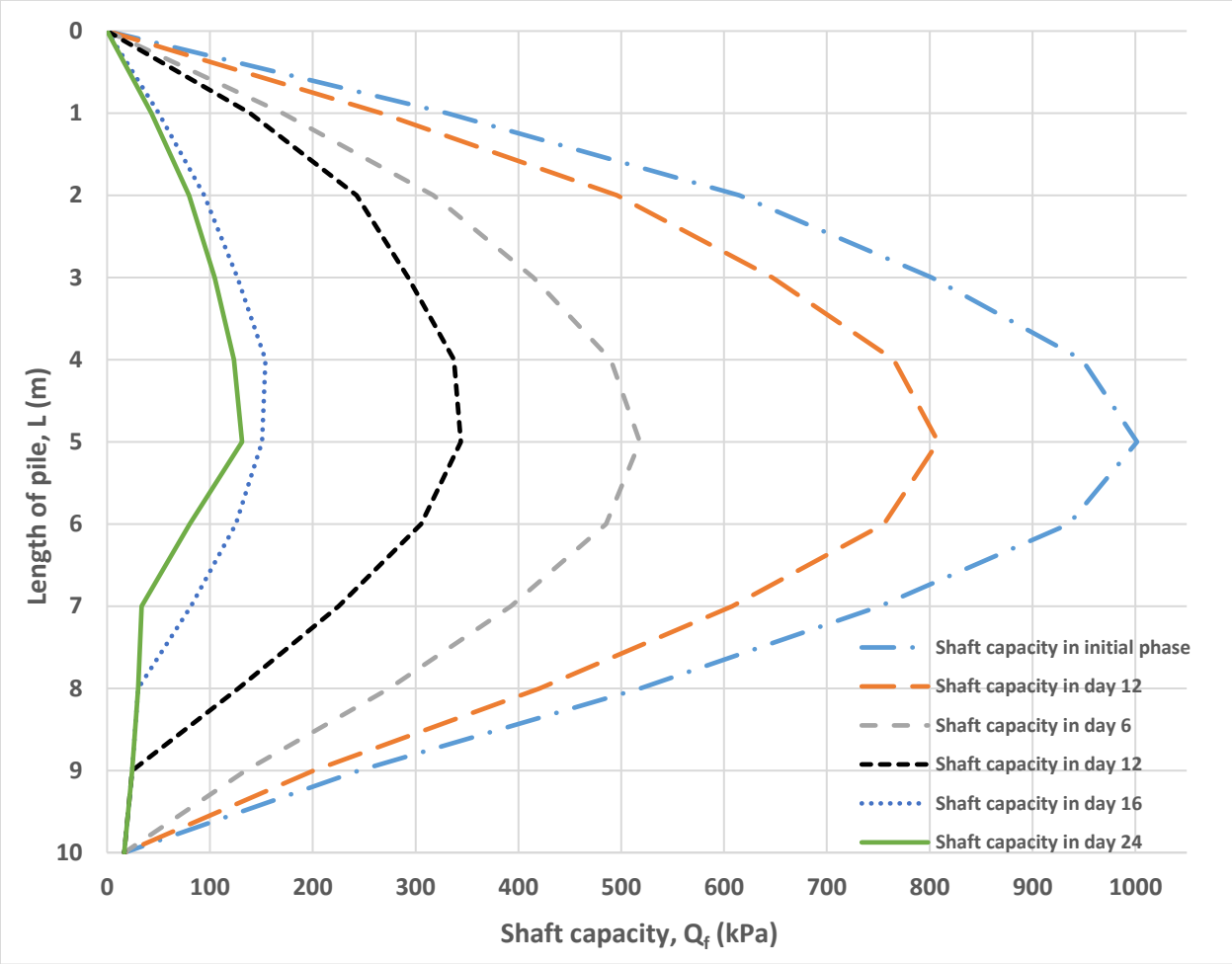

Figure 4-27 Analytical calculation result of sand shaft capacity after rainfall using modified lambda method

4.4.2 Result of numerical analyses for fine-grained soil (Kaolin):

Table 4-8 Laboratory data used for foundation modeled in Kaolin soil using plaxis

Soil type	Kaolin
Soil Model	Mohr-Coulomb
Drainage Type	Drained
Unsaturated unit weight	18.3 KN/ m^3
Saturated unit weight	20.83 KN/ m^3
Void ratio	0.2
Modules of elasticity	15.76 KN/ m^3
Cohesion	18
Friction angle	14

Plaxis 3D was used to examine the variation in suction for fine-grained soil caused by rainfall. For the sake of this computation, a 10m pile length is used. 12 days of rain are followed by 12 days without rain. The volume of rainfall and the time interval of rainfall may both be added in the stage creation step of modeling using Plaxis. According to the outcome of the numerical calculations, rainfall penetration in both fine- and coarse-grained soil causes a decrease in suction. For coarse-grained soil (Sand), the initial suction is 100 kPa (before rainfall infiltration), declining to 92 kPa after one day of continuous rain, 34 kPa after 12 days of rain, and 13 kPa after the period. This shows that even after 12 days of rain, water continues to flow into the water table, lowering the negative pore water pressure. Additionally, due to rainfall, the groundwater table depth decreases from its original assumption of 10 meters to 9 meters after the time. The outcome also shows that soil would weaken as a result of reduced suction.

Figure 4-28 displays a 3D representation of the foundation as well as a cross-section of a pile that was designed using Plaxis 3D. The pile's cross-section shows that rainwater in the kaolin causes the matric suction to diminish. Before the rain, it was 100 KPa, and by the conclusion of the period under consideration, it was 12 KPa. Additionally, it demonstrates how, as a result of water infiltration at the groundwater table and into the depths, the negative pore water pressure decreases during the 12 days of the dry time that follow the 12 days of rainfall.

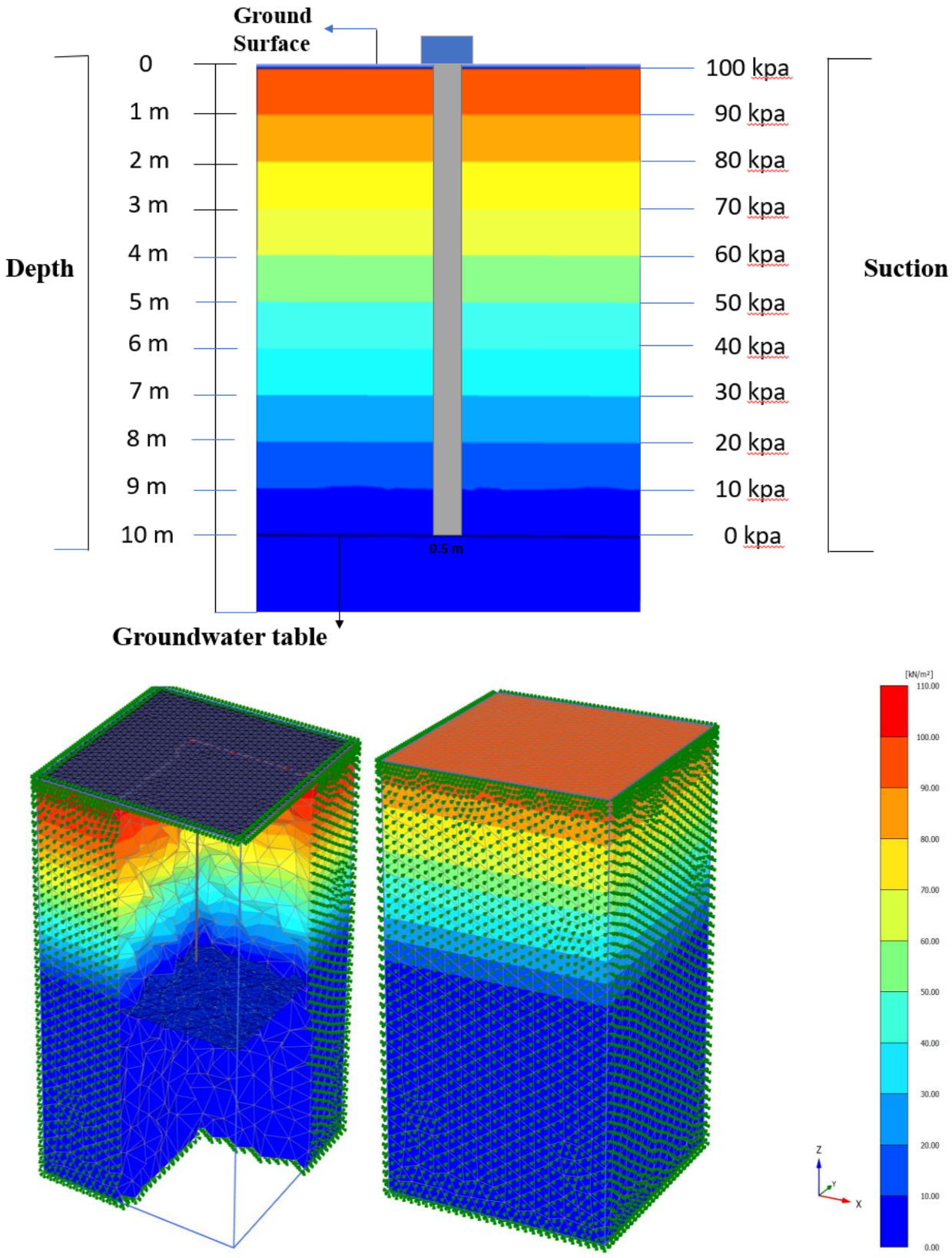

Figure 4-28 Initial phase in plaxis 3D analyses

Figure 4-29 illustrates the suction changes to 33 KPa after 12 days of rainfall at the ground surface and it declines to 0 KPa at depth of 10m of the groundwater table. This suction reduction causes the shaft capacity of the pile to decrease.

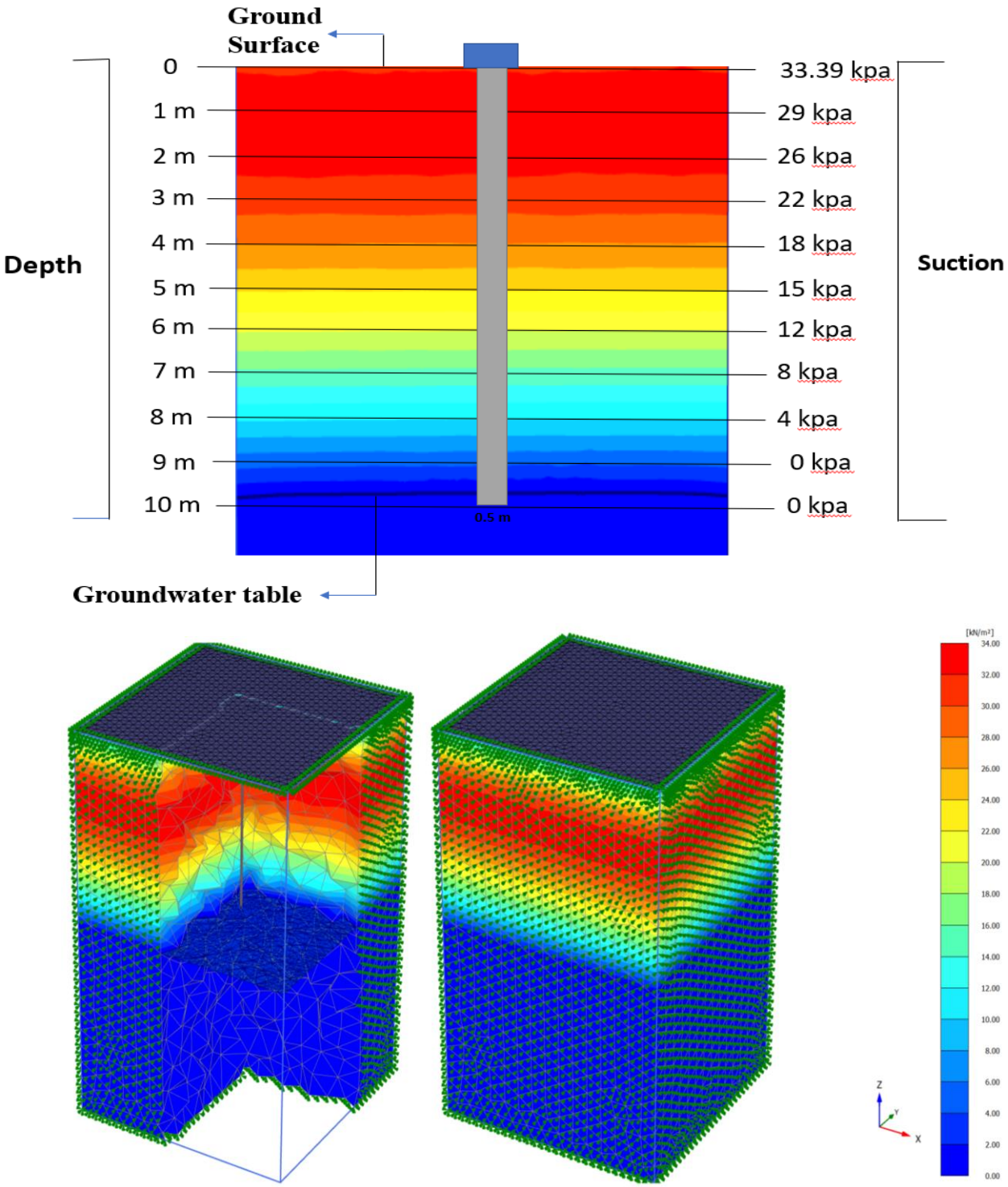

Figure 4-29 Suction variation of Kaolin due to rainfall in plaxis 3D analyses

the negative pore water pressure (matric suction) diminishes with rainfall and the subsequent dry interval. This is seen in Figure 4-30. In the first phase, the suction is operating at its maximum rate of 100 KPa. (day 0). It descends in a downward direction until it hits 12 KPa after the time. The suction fluctuation caused by rainfall in the fine-grained soil over the course of 12 days is shown in Figure 4-31. According to the graph, there is a 34 kPa maximum suction after 12 days of rain. The suction changes throughout the 12 days following a downpour are shown in Figure 4-32. According to the graph, the maximum suction after the dry time of 12 days is 12 kPa. After 12 days of rainfall, the soil suction drops from 100 kPa to 34 kPa, and then it drops to 12 kPa after the time, showing a 66 kPa reduction in 12 days of rainfall and an 88 kPa reduction in the whole 15-day period.

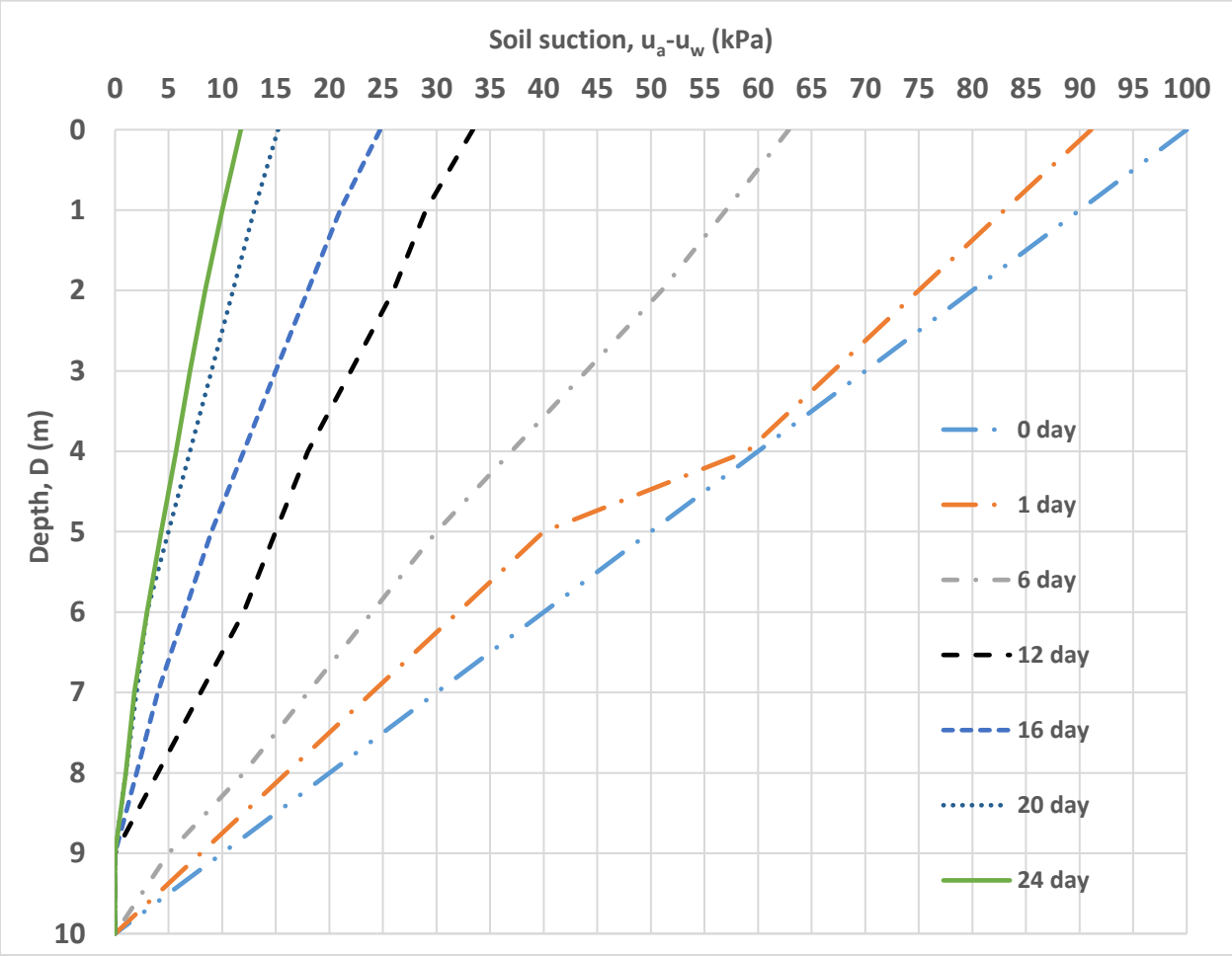

Figure 4-30 Graph of suction variation of Kaolin due to rainfall in plaxis 3D analyses

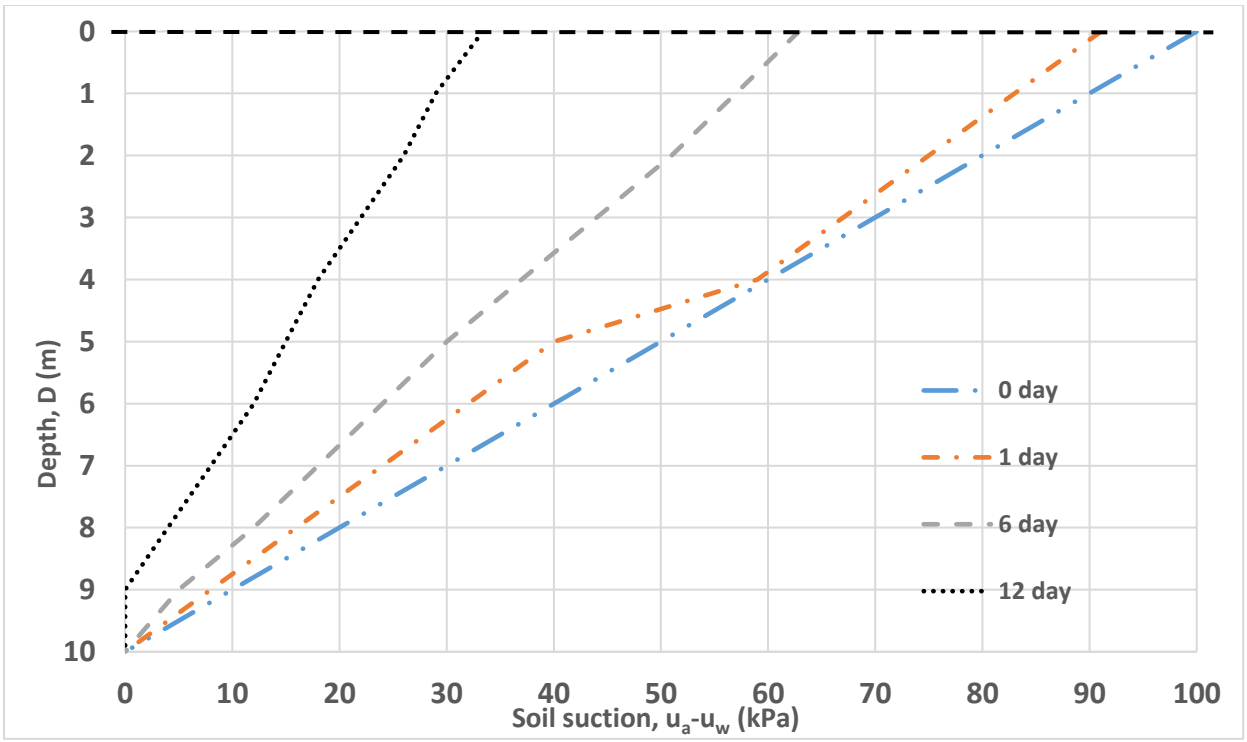

Figure 4-31 Graph of suction variation of Kaolin due to 12 days of rainfall in plaxis 3D

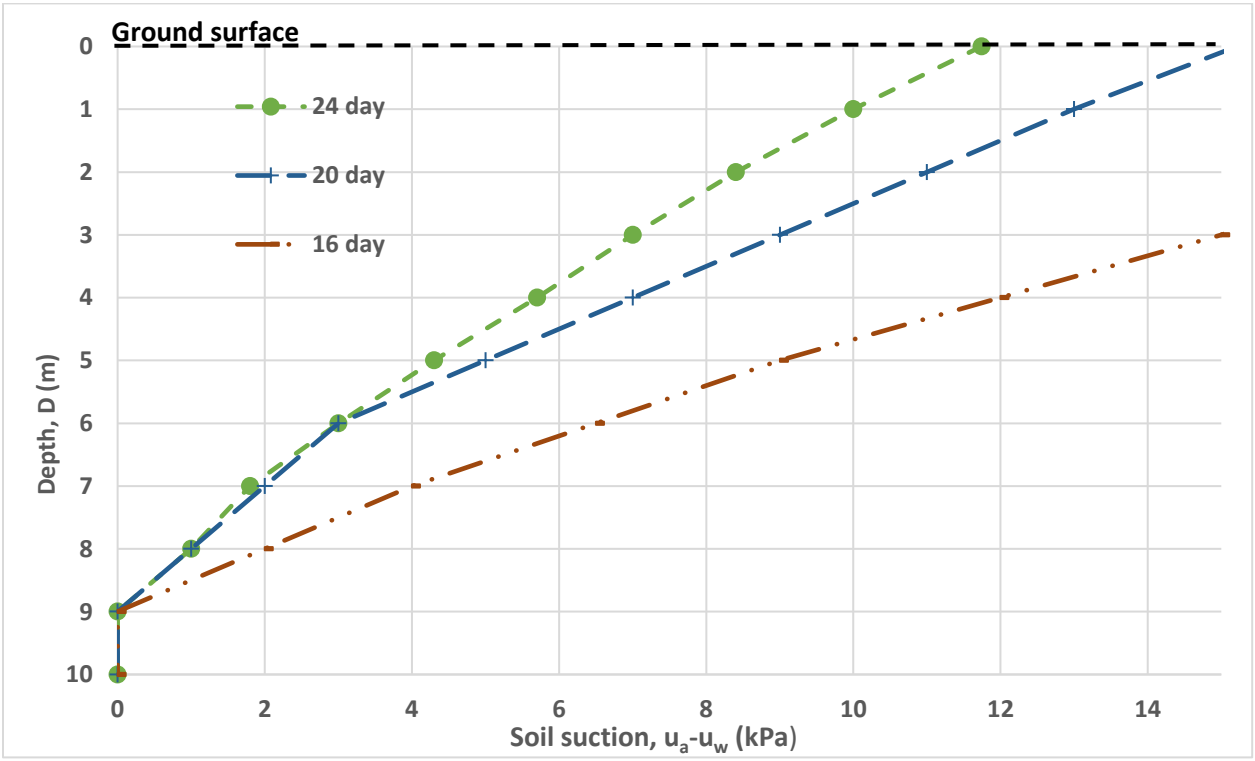

Figure 4-32 Graph of suction variation of Kaolin due to 12 days of dry period in plaxis

4.4.2.1 Shaft capacity of the pile after rainfall infiltration from plaxis results for fine-grained soil (kaolin):

4.4.2.1.1 Modified Beta Method:

Figure 4-33 displays the results of an analytical computation using the modified Beta approach. The calculations were done in a 10 m groundwater table and 10 m length of pile for the initial phase (before rainfall), Day 1, Day 6, Day 12, Day 16, and Day 24. The modified beta method's findings show that rainwater infiltration causes the shaft capacity of pile foundations with fine-grained soil (kaolin) to decrease by 45 KPa, going from 320 KPa in the first phase to 275 KPa after the 12-day rainy period. In the dry period following a rainstorm, the shaft capacity of a pile within kaolin soil reduces from 275 KPa to 155 KPa.

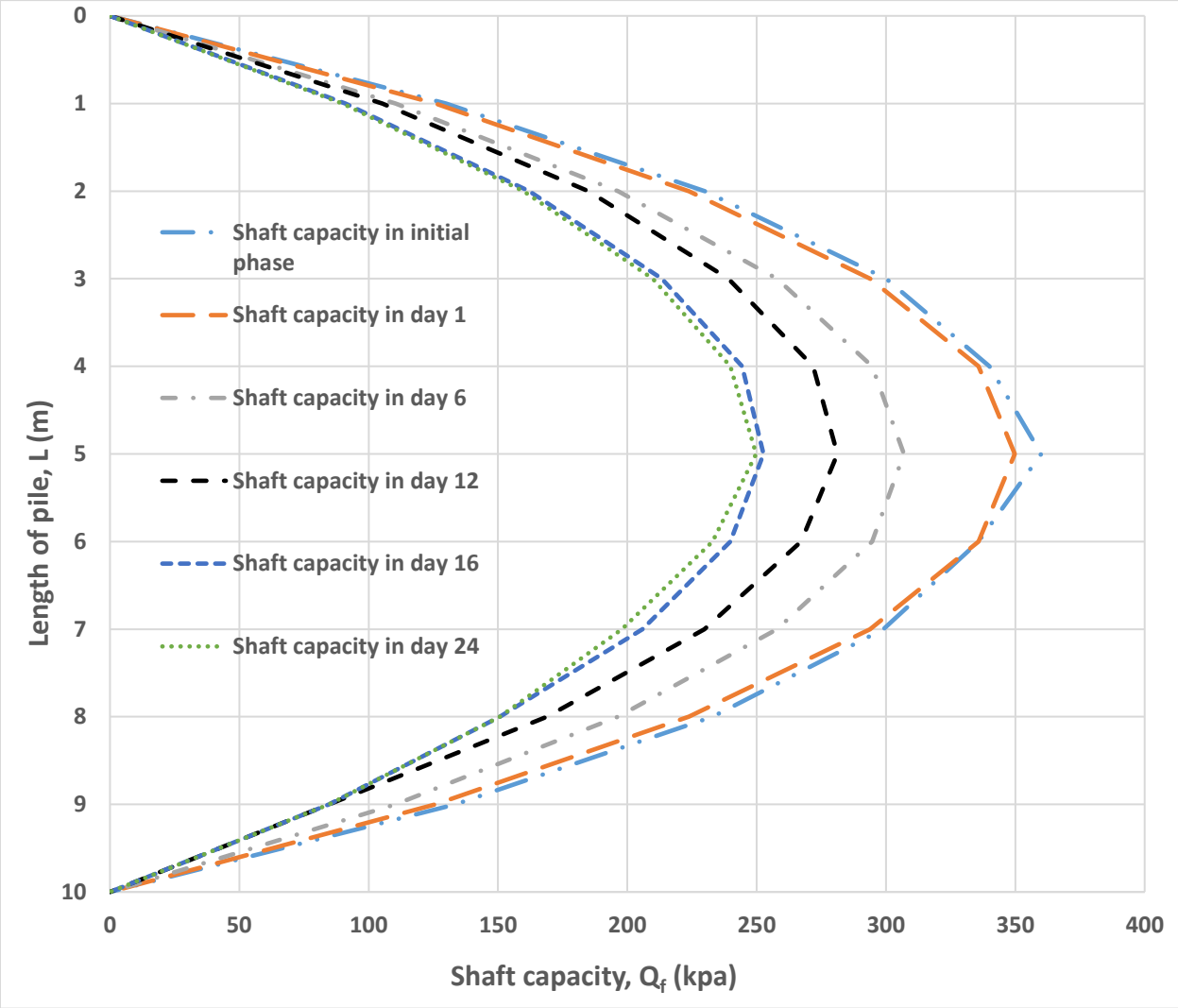

Figure 4-33 Analytical calculation result of kaolin shaft capacity after rainfall using the modified beta method

4.4.2.1.2 Modified Alpha Method:

calculations were done in 10 m of groundwater table depth and 10 m of pile length for the first phase (before rainfall), Day 1, Day 6, Day 12, Day 16, and Day 24. According to the modified alpha method's findings, the shaft capacity of pile foundations decreases by 120 KPa as a result of rainwater infiltration, going from 170 KPa during the first phase to 50 KPa after 12 days of rain. In the 12 days of the dry season, the shaft capacity of the pile foundation in the kaolin soil falls. It decreases from 50 KPa to 20 KPa, a difference of 30 KPa.

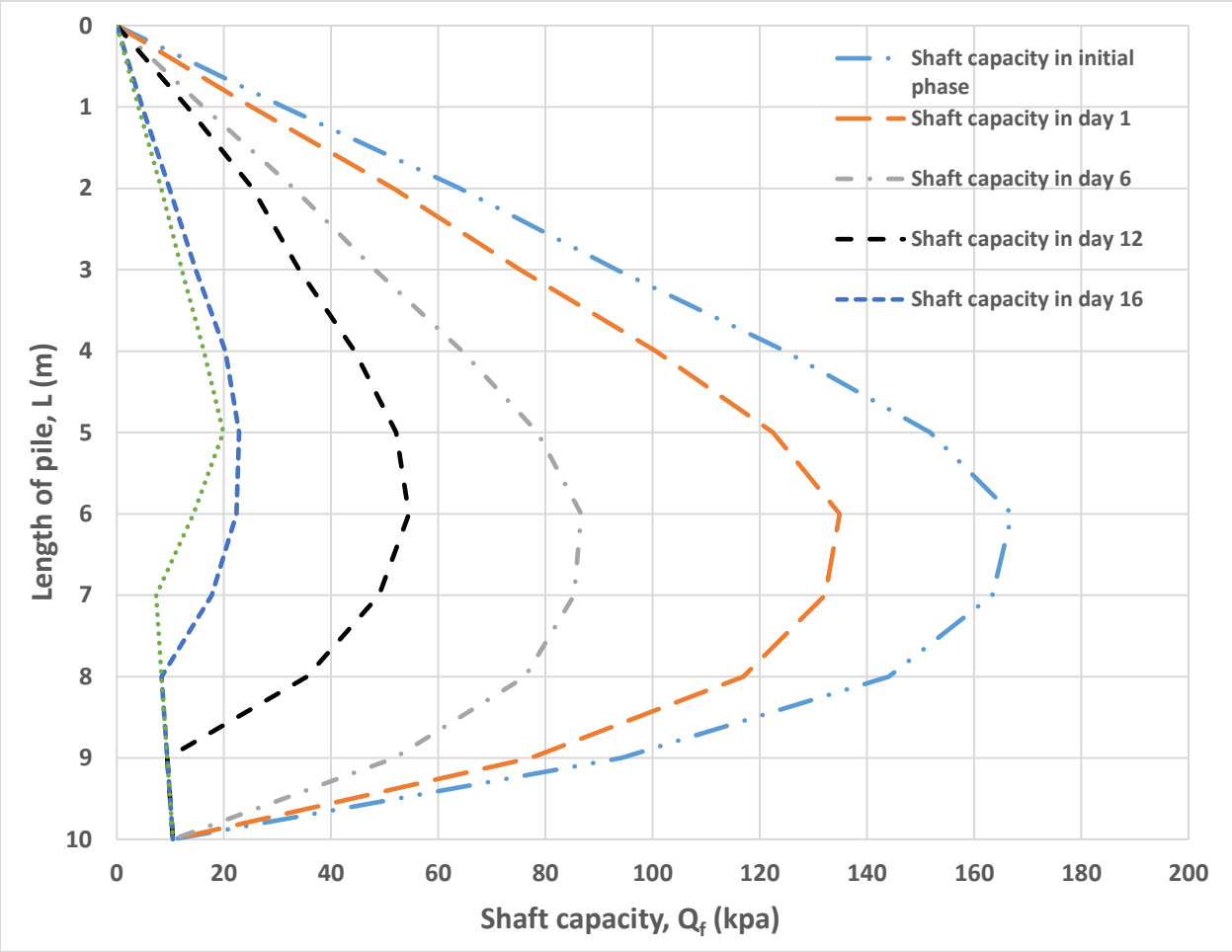

Figure 4-34 Analytical calculation result of kaolin shaft capacity after rainfall using the modified beta method

4.4.2.1.3 Modified Lambda Method:

The results of an analytical computation utilizing the modified lambda approach are shown in Figure 4-35. The calculations were done in 10 m of groundwater table depth and 10 m of pile length for the first phase (before rainfall), Day 1, Day 6, Day 12, Day 16, and Day 24. The modified beta method's findings show that rainwater infiltration causes the shaft capacity of pile foundations in fine-grained soil (Kaolin) to decrease by 820 KPa, going from 1000 KPa in the first phase to almost 180 after the rainy period. Due to reduced suction, the pile's shaft capacity will continue to decline over the dry period. It changes from 180 KPa to 70 KPa, which is a change of 110 KPa.

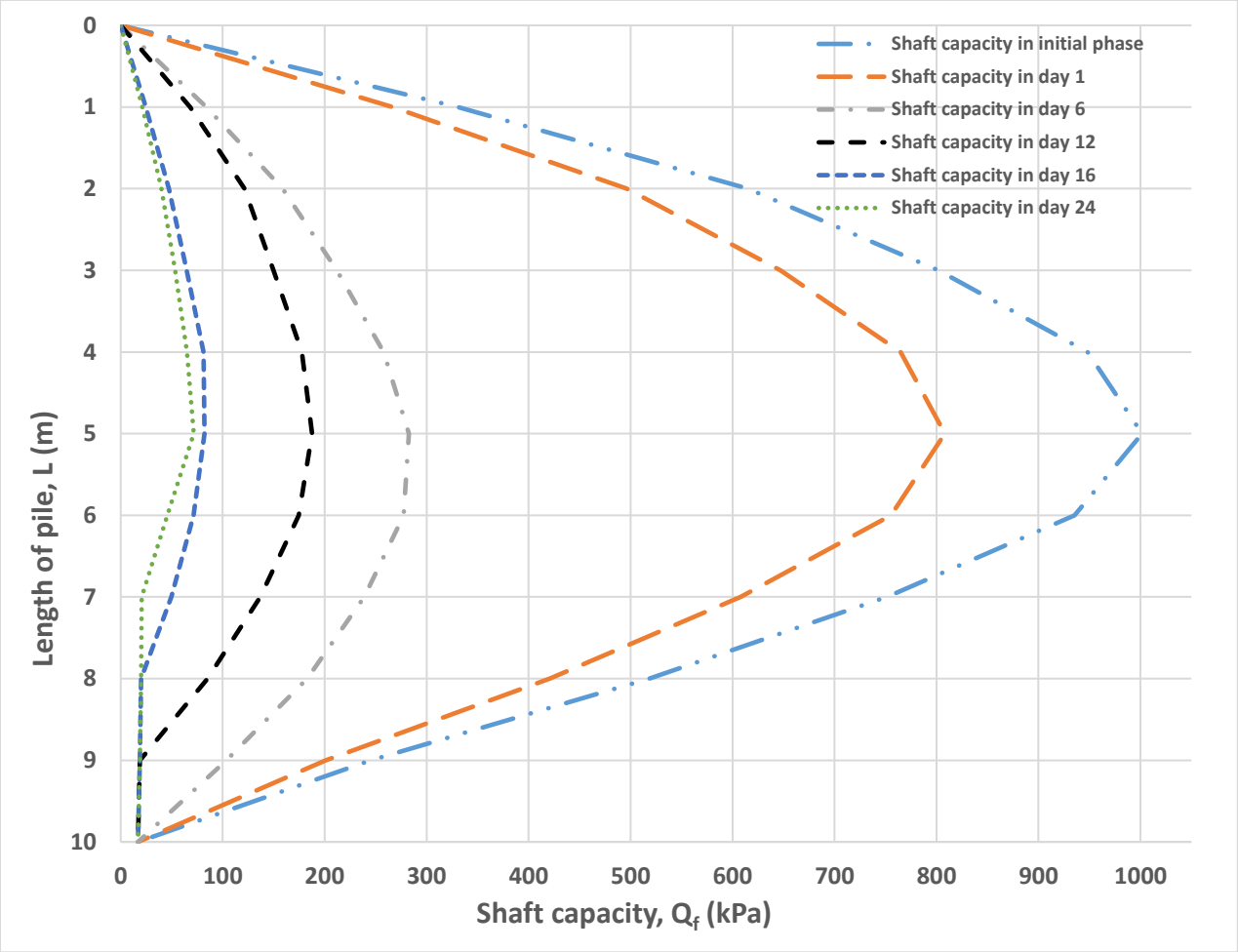

Figure 4-35 Analytical calculation result of kaolin shaft capacity after rainfall using modified lambda method

Chapter 5 Conclusion

Unsaturated soil mechanics creates a larger shaft capacity for pile foundations, per the findings of the current thesis work. Rainfall also weakens the suction in the soil, which lowers the pile foundation's shaft capacity in both coarse- and fine-grained soil (sand) (kaolin). Concerning matric suction and rainwater infiltration, the conventional and modified, and techniques are used to calculate the shaft capacity of the pile.

Below is an overview of the comparisons and assessments for kaolin (fine-grained soil) and sand (coarse-grained soil):

1. The laboratory data from the hyprop test shows that the sands air entry value (AEV1) happens in 20 KPa suction whereas kaolin's happens in less than100 KPa suction.
2. Fine-grained soil (Kaolin) shows lower permeability compare to coarse-grained soil (sand). According to the results, the permeability of the sand is around 0.02 m/s however the permeability of the kaolin is 0.000006 m/s.
3. Result from analytical calculation shows that modified methods incorporating the negative pore water pressure produce higher shaft capacity of pile foundation in all three methods alpha, beta, and lambda. For instance, for a 10-meter depth of groundwater table in coarse-grained soil for 10 m length of pile shaft capacity is 1180 KPa, 60 KPa, and 320 KPa in conventional beta, alpha, and lambda methods whereas 1280 KPa, 135 KPa, and 570 KPa in modified beta, alpha, and lambda methods respectively which shows a 100 KPa, 165 KPa and 160 KPa differences between two methods. Similarly for 10-meter depth of groundwater table in fine-grained soil and 10-meter length of pile shaft capacity is 150 KPa, 60 KPa, and 190 KPa in conventional beta, alpha, and lambda methods whereas it is 340 KPa, 136 KPa, and 440 KPa in modified beta, alpha and lambda methods respectively which indicates a 100, 165 and 160 KPa between two methods. The differences between the three methods are the same for both types of soil. Based on the above outcomes, unsaturated soil utilization is recommended in foundation design for higher shaft capacity and pile optimization.
4. Results from numerical analyses demonstrate that rainfall has a considerable effect on the reduction of pile shaft capacity due to suction variation within the fine- and coarse-grained soil. The outcome from plaxis 3D analyses shows that the suction within the coarse-grained soil decreases from 100 KPa before the rainfall to 80 KPa on first day of rainfall and to 30 kPa after 12 days of rainfall (the amount of rainfall is 20mm per day) and continues to decline to 10 kPa at the end of 15 days period. Similarly, the analyses indicate that the suction within the fine-grained soil decreases from 100 kPa in the day before the rainfall to 90 kPa in the first day of rainfall and to 34 kPa after 12 days of rainfall and continues to decline to 12 kPa at the end of 15 days period.
5. The suction within the course-grained soil (sand) decreases by 70% in 12 days of rainfall and similarly continues to decrease by 20% in 12 days of dry period. Overall, it falls by 90% in 15 days period. The same trend with the fine-grained soil, the suction decreases by 66% in 12 days of rainfall and similarly continues to decreases by 13% in 12 days of dry periods. Overall, it falls by 88% in 15 days period.
6. The result of suction variation from numerical analyses is used in the analytical calculation using modified alpha, beta, and lambda to calculate the shaft capacity of the pile after rainfall infiltration within the fine- and

coarse-grained soil. The outcome provides us with information which the shaft capacity of the pile declines with the soil suction. For instance, the shaft capacity of a 10-meter pile in a coarse-grained soil reduces from 1280 KPa to 1120 (beta method) 168 to 44 (Alpha method), and 1000 to 350 (Lambda method) during 12 days of rainfall. Similarly, the shaft capacity of a 10-meter pile in fine-grained soil reduces from 320 KPa to 275 (beta method) 170 to 50 (Alpha method), and 1000 to 180 (Lambda method) during 12 days of rainfall. According to the results, the pile foundation within course-grained soil has higher shaft capacity compared to fine-grained soil.

shaft capacity of the pile calculated by the modified beta method is higher compared to modified alpha and modified lambda and it is due influence of effective stress in this method.

REFERENCES

Baymahan, A.R., Baymahan, R.B., Kalimoldayev, M.N. (2015). Development of plasticity conditions for a sub-fundament soil base of the anisotropic structure. Stroitel'nyye konstruktsii i materialy, (57), (in Russian). Retrieved from http://rmebrk.kz/journals/1548/36472.pdf

Buranbayeva, A. M., Zhussupbekov, A. & Omarov, A.R. (2012). Numerical analysis and geo monitoring of the behavior of the foundation of Abu-Dhabi Plaza in Astana. Journal of Physics: Conference Series.

Fredlund DG, Slope stability hazard management systems. SCIENCE A, 8(11):1695-1711. Fredlund DG, 2007. https://doi.org/10.1631/jzus.2007.A1695

Fredlund et al., D.G. Fredlund, H. Rahardjo, M.D. Fredlund Unsaturated Soil Mechanics in Engineering Practice John Wiley & Sons Inc, New York (2012), p. 917

Fredlund, D.G. and H. Rahardjo (1993) "Soil Mechanics for Unsaturated Soils". John Wiley & Sons, Inc., New York, 517 pages (ISBN 0-471-85008-X).

Fredlund, D.G., H. Rahardjo and M.D. Fredlund (2012). "Unsaturated Soil Mechanics in Engineering Practice". John Wiley & Sons, Inc., New York, 917 pages (ISBN 978-1-118-13359-0).

Fredlund, D.G., Sheng, D. and Zhao, J. (2011). Estimation of soil suction from the soil-water characteristic curve. Canadian geotechnical journal, 48(2), pp.186-198.

Khomyakov, V. A., Iskakov, E. E., & Serdaliev, E. T. (2013). Investigation of Gravelly Soil During Underground Construction in Almaty. Soil Mechanics and Foundation Engineering, 50(4), pp. 171–177. doi:10.1007/s11204-013-9140-z

Kim, Y., Satyanaga, A., Rahardjo, H., Park, H. and Sham, A.W.L. (2012) “Estimation of effective cohesion using artificial neural networks based on index soil properties: a Singapore case” Engineering Geology, August, vol. 289, No 106163.

Kristo, C., Rahardjo, H. and Satyanaga, A. (2019) “Effect of Hysteresis on The Stability of Residual Soil Slope”. International Soil and Water Conservation Research. September 2019. Vol. 7, pp. 136-148. https://doi.org/10.1016/j.iswcr.2019.05.003

Mercer, K., Rahardjo, H., Satyanaga, A. (2019). Soil–Water Characteristic Curves for Materials Classified According to the Unified Soil Classification System. ISBN 978-0-9876389-0-8.

Morris, P. H., Graham, J., & Williams, D. J. (1992). Cracking in drying soils. Canadian Geotechnical Journal, 29(2), pp.173-277.

Pachikin, K., Erokhina, O., & Funakawa, S. (2013). Soils of Kazakhstan, Their Distribution and Mapping. Environmental Science and Engineering, pp.519–533.

Rahardjo H, Satyanaga A, D'Amore GAR, et al. Soil-water characteristic curves of gap-graded soils. Engineering Geology, 116:102-107, Singapore, 2012 https://doi.org/10.1016/j.enggeo.2011.11.009

Rahardjo, H., A. Satyanaga and E.C. Leong (2012) "Unsaturated Soil Mechanics for Slope Stabilization.". Southeast Asian Geotechnical Journal, March, Vol. 43, No.1, pp. 48-58.

Rahardjo, H., A. Satyanaga, F.R. Harnas and E.C. Leong (2016a). "Use of Dual Capillary Barrier as Cover System for a Sanitary Landfill in Singapore". Indian Geotechnical Journal, September, Vol. 46, No. 3, pp. 138-148.

Rahardjo, H., N. Gofar, F. Harnas, and A. Satyanaga (2018) "Effect of Geobags on Water Flow through Capillary Barrier System", Southeast Asian Geotechnical Journal, Vol. 49(4).

Rahardjo, H., Satyanaga, A. & Leong, E.C. (2016b). "Effects of rainfall characteristics on the stability of tropical residual soil slope." Proceedings of E-UNSAT 2016, E3S Web of conferences 9, Sep 2016, 15004, 1-6, DOI:10.1051/e3sconf/20160915004.

Rahardjo, H., Satyanaga, A., Leong, E.C., Ng, Y.S. Variability of residual soil properties. Eng. Geol., 2012, 141–142(115–140).

Satyanaga A, Rahardjo H, Zhai Q, Estimation of unimodal water characteristic curve for gap-graded soil. Soils and Foundations, 57:789-801., Singapore , 2017 https://doi.org/10.1016/j.sandf.2017.08.009

Satyanaga, A., Bairakhmetov, N., Kim, J.R. & Moon, S.-W. (2013) Role of bimodal water retention curve on the unsaturated shear strength. Applied Sciences. 12(3), 1176. https://doi.org/10.3390/app12031176

Satyanaga, A., Kim, J., Moon, S., Wijaya, M. (2020). Exponential Functions for Modeling Hysteresis of Soil-Water Characteristic Curves. E3S Web of Conferences, 195. doi.org/10.1051/e3sconf/202019502002

Vanapalli SK, Garga VK, Brisson P, A modified permeameter for determination of unsaturated coefficient of permeability. Geotechnical and Geological Engineering, 16(2):191-202, 2007. https://doi.org/10.1007/s10706-006-9103-6